

An Improved Wild Horse Optimization algorithm for Reliability Based Optimal DG Planning of Radial Distribution Networks

Mohammed Hamouda Ali¹, Salah Kamel², Mohamed H. Hassan², Marcos Tostado-Véliz³, Hossam M. Zawbaa^{4,5,*}

¹Department of Electrical Engineering, Faculty of Engineering, AL-Azhar University, Cairo, 11651, Egypt; Eng_MohammedHamouda@azhar.edu.eg (M.H.A.).

²Department of Electrical Engineering, Faculty of Energy Engineering, Aswan University, Aswan 81528, Egypt; skamel@aswu.edu.eg (S.K.); mohamedhosnymoe@gmail.com (M.H.H.).

³Electrical Engineering Department, University of Jaen, EPS, 23700 Linares, Spain; mtostado@ujaen.es (M.T.-V.)

⁴Faculty of Computers and Artificial Intelligence, Beni-Suef University, Beni-Suef, Egypt

⁵Technological University Dublin, Dublin, Ireland; hossam.zawbaa@gmail.com

Abstract: This paper introduces a novel technique for optimal distribution system (DS) planning with distributed generation (DG) systems. It is being done to see how active and reactive power injections affect the system's voltage profile and energy losses. DG penetration in the power systems is one approach that has several advantages such as peak savings, loss lessening, voltage profile amelioration. It also intends to increase system reliability, stability, and security. The main goal of optimal distributed generation (ODG) is a guarantee to achieve the benefits mentioned previously to increase the overall system efficiency. For extremely vast and complicated systems, analytical approaches are not suitable and insufficient. Therefore, several meta-heuristic techniques are favored to obtain better performance from where convergence and accuracy for large systems. In this paper, an Improved Wild Horse Optimization algorithm (IWHO) is proposed as a novel metaheuristic method for solving optimization issues in electrical power systems. IWHO is devised with inspirations from the social life behavior of wild horses. The suggested method is based on the horse's decency. Reliability amelioration is the most things superb as a result of DGs incorporation. Thus, in this research, a customer-side reliability appraisal in the DS that having a DG unit was carried out by a Monte Carlo Simulation (MCS) approach to construct an artificial history for each ingredient across simulation duration. For load flow calculations, the backward Forward Sweep (BFS) technique has been employed as a simulation tool to assess the network performance considering the power handling restrictions. The proposed IWHO method has been measured on IEEE 33 and 69 buses to ascertain the network performing in the presence of the optimal DG and the potential benefits of the suggested technique for enhancing the tools used by operators and planners to maintain system reliability and efficiency. The results proved that IWHO is an optimization method with lofty performance regarding the exploration-exploitation balance and convergence speed, as it successfully handles complicated problems.

39 **Keywords:** Radial Distribution Network, Distributed Generation, BFS Algorithm, Improved wild
40 horse optimization algorithm, Reliability assessment, Monte Carlo simulation.

41

42 **1. Introduction**

43 Nowadays, there is a global unanimity that incorporating renewable energy sources (RESs) as
44 distributed generators (DG) is crucial to facing the rising electricity need and reducing the overall
45 carbon dioxide footprint. It is one of the most successful and realistic planning methods for enhancing
46 the network's reliability and power quality as demand increases. The DG penetration strategy in the
47 DS is becoming more common as demand load increases, pollutant emissions are reduced, and the
48 electrical power market is deregulated [1]. The leverage of DG performance is more closely related to
49 the types, locations, and sizes of the DG units used, where the best choice will maximize the benefits
50 of the DG units while avoiding their downsides for the system, such as voltage volatility, increased
51 system loss and increased operating costs [2, 3]. The effects of including DG units into the system
52 vary depending on whether the system is in steady-state or transient mode. Some issues occur in the
53 steady-state, such as extreme energy losses, reverse current flow, fluctuations in voltage, managing
54 reactive power, malfunction in the protective system, and weak power quality. [4–6]. The conse-
55 quences in the transitional state are, on the other hand, caused by the separating DG units and the
56 unexpected outputs of the DG units, such as fluctuations in wind speed and solar radiation. [7]. The
57 acuity of these effects is based on the placement of DG units, the DG penetration levels, and the sort
58 of DG. Furthermore, owing to the nature of renewable DG units, simultaneous fluctuations in DG
59 generation for providing the demand load might lead to a down or overvoltage. The implications of
60 such events may be altered by the placement of DG units and weather conditions, as mentioned previ-
61 ously [8]. Additionally, the system performance is enhanced at the particular penetration levels of the
62 DG units, while the system was in contrast degraded by substation and feeder load, voltage devia-
63 tions, and higher power losses beyond this level. As a result, the ODG allocation problem has recently
64 piqued the interest of many researchers to achieve various goals, including minimizing real power
65 loss, enhancing voltage profile, boosting power quality, and mounting the distribution system's relia-
66 bility and efficiency. As a result, many ways to addressing these issues have been proposed in the
67 literature. A mixing of analytical approach and heuristic search has been suggested for optimal place-
68 ment of DGs in the DS for minimizing power loss in [9]. An efficient analysis (EA) approach to
69 properly deploy multiple DG units is presented to reduce power loss in distribution systems[10]. A
70 novel approach for determining the optimum size and the location of DG was presented in [11] to
71 reduce the power loss and ensure the system's voltage stability. In [12], the authors used an enhanced
72 gravitational search algorithm to learn the location and dimensions of photovoltaics (PV) based DGs
73 to reduce overall expenditures. In[13], the authors presented a technique that would increase the glob-
74 al seeking ability, called Quasi-Oppositional Chaotic Symbiotic Organisms Search (QOCSOS). The

75 goal of this work is to curb the power loss, enhance the voltage profile, and raise the voltage stability
76 in the radial distribution networks (RDNs). Mixed-integer nonlinear programming (MINLP) tech-
77 nique has been utilized in [14] to identify the best size and position of DGs with power loss curtail-
78 ment. In [15], the Electrostatic Discharge Algorithm (ESDA) was utilized to resolve the problem of
79 DG assignment to augment the voltage stability and limit the power losses. To optimize the allocation
80 of DGs in the DS concerning reducing annum power losses, the authors are introduced an artificial
81 ecosystem-based technique [16]. To decrease power loss in DS, a simplified analytical technique was
82 presented for optimum DG amalgamation in [17]. The aim of [18] is for an ODG allocation in the
83 typical IEEE 33-bus system to promote voltage stability and minify total power loss. This is based on
84 the Gray Wolf optimization method with loss sensitivities. The Ant Lion Optimization Algorithm
85 (ALOA) is presented in [19] for ODG allocation of RDG sources in diverse RDNs. In [20], the au-
86 thors offer a hybrid approach based on the combined power loss sensitivity (CPLS) and Salp Swarm
87 Algorithm (SSA) to merge PV and wind turbines (WT) in the DS for boosting voltage, reducing loss-
88 es, and expanding system capacity. The purpose of [21] is to resolve the best allocation of the DGs in
89 a RDN, diminish the overall operational costs and voltage indexes variations, and ensure a more flex-
90 ible solution of the hybrid fuzzy logic controller technique and the particle swarm optimization (PSO)
91 with the ALOA. The authors utilized the LSF in [22, 23] to locate the elected bus. To mend the volt-
92 age profile and decrease the power loss of the RDN, simulated annealing (SA) and PSO were used to
93 set the optimal position and size of DG. The SAPSO approach to banning the SA & PSO shortage by
94 two methods was introduced and produced the finest solutions in a short time. This article [24] pro-
95 vides an application for optimal sizing and positioning of RDGs including WT, PV, and biomass in
96 DS using a new metaheuristic rider optimization algorithm (ROA).

97 To epitomize, an improved wild horse optimization algorithm (IWHO) is suggested as a novel
98 population-based algorithm to compete with state-of-the-art and neoteric optimization algorithms. It
99 should be evident that the intended algorithm provides the poise between exploration and exploitation.
100 This feature enables IWHO to solve a complicated optimization issue with multiple locally optimal
101 solutions because it retains several answers and explores a broad area to pinpoint the global solution.
102 Finally, the IWHO is the greatest and most innovative approach for optimizing problems because of
103 loud fineness and soft calculations. To sum up, this research's key contributions are:

104 Introduce for the first time in the power system a devise approach called an improved wild horse
105 optimization algorithm (IWHO) to augment search quality and shun an early convergence to a local
106 minimum.

107 Proposed the optimal option of the ODG allocation (size & position) considering the constraints of the
108 RDN. Standard IEEE 33 & 69 bus networks are hired to check the leverage of the suggested algo-
109 rithm.

130 Demonstrated the efficacy of the outcomes of this approach in terms of lowering losses and meliora-
111 tive the voltage profile.

142 Verified the performance of the methodology proposed using typical test systems to detect its
113 superiority for handling the problems and compared to other published approaches.

154 An artificial history for each component in the test system is generated using MCS instead of an
115 analytical method for highly efficient reliability assessment.

116 This paper was structured as follows: Section 2 depicts the BFS algorithm. The mathematical de-
117 scription of the optimization problem is described in Section 3. Section 4 focuses on the IWHO algo-
118 rithm. Section 5 transact with the simulation results for the test systems and discussion. Finally, in
119 Section 6, the suggested work's inference is provided.

120 **2. Backward Forward Sweep Algorithm**

121 Load flow is a crucial tool for the design, and operation of power systems to guaran-
122 tee reliability, stability, and economy. Classical methods as gauss-seidel (GS) and newton raphson
123 (NR) might be inappropriate for the DS and diverge because of [23]:

124 Radial formation.

125 R/X value is higher.

126 Running lopsided.

127 DGs.

128 Backward/Forward Sweep (BFS) is chosen for fit planning owing to:

129 The poor nature of RDS.

130 Accurate load flow results rely on convergence, simulation time, and the convergence rate.

131 This technique is carried out through two phases: rear and front sweep using the demand and
132 streak data as follow:

133 *2.1. Forward Sweep*

134 In essence, a voltage decline is calculated through branch currents. Node voltages are updated
135 from the first bus to the most distant bus. The fore scanning aims to identify the node voltage for all
136 buses starting from the origin node. The primary bus voltage is set to 1pu, and the current in reverse
137 propagation is firm.

138

139

140 *2.2. Backward Sweep*

141 It is mainly a voltage upgraded by a load flow computation. It moves from the furthest lines to
 142 the head node. In the rear-prevalence count, the updated current flows are achieved utilizing the bus
 143 voltage of the previous rounds. It implies that the voltage values obtained are not changed during the
 144 rear prevalence computations in the front prevalence.

145 The BFS algorithm steps are listed below:

- 146 • Set the injected current ($I_i = 0$)
- 147 • Set all nodes voltage ($V_i = 1 \text{ pu}$)
- 148 • Compute the node current ($I_i = \frac{S_i^*}{V_i^*}$)
- 149 • Evaluate current of the lines (backward sweep)

$$150 \quad I_{(i,i+1)} = I_{i+1} + \sum (\text{branches current at node } i + 1)$$

- 151 • Modernizing the voltage of buses ($V_i = V_{i+1} + (Z_{(i,i+1)} * I_{(i,i+1)})$)
- 152 • Until the criteria are terminated.

153 3. Problem Formulation

154 The main key for a healthy environment is renewable distribution generation (RDG), which plays
 155 a main role in power systems. Tentatively, the peril of fuel price swings and political influences
 156 should be decreased by incorporating the RDGs and guaranteeing that these do not significantly influ-
 157 ence public well-being overall. In such regard, changes to the grid might be necessary due to modify
 158 the choices of generating sources, which is caused by a large amalgamation of RDGs. The fluctuation
 159 of current and voltage in the network is increased as a result of DG permeation. Increasing DG per-
 160 meation might therefore have a detrimental or beneficial influence depending on the scale of the sys-
 161 tem and the sort of the load, necessitating modeling and emulation to evaluate its action. If not ade-
 162 quately striped, this may result in an unforeseen rise in power flow, leading to network crowding and
 163 higher network losses. DGs offer significant advantages for terminus consumers and their technical
 164 assistance through increased reliability, power quality, and cost dilution. Cost cuts and the pressing
 165 requirement to fuse DGs maybe drive energy demand. Therefore, good system planning is significant
 166 for the good running of the entire system. This concerns the development of convenient mathematical
 167 models and algorithms that allow for optimum positioning and size of DGs in the system; this is the
 168 issue handled in this study.

169 3.1. Objective Function (OF)

170 Its major aim is to identify the best localization and sizing of DGs to constrict the total losses in
 171 light of equity and inequality restrictions., which can be described as follow:

$$OF = \min(P_{loss}) = \min \sum_{i=1}^L R_i \left(\frac{P_i^2 + Q_i^2}{V_i^2} \right) \quad (1)$$

172 3.2. Constraints

173 The limits ensuring the superior performance of the RDGs technology are split into operating and
174 technological restrictions as see:

175 3.2.1. Operational constraints

176 These are called the equality restriction and apportioned into:

177 Power balance constraints

$$P_i = |V_i| \sum_{j=1}^N |V_j| \times |Y_{ij}| \times \cos(\theta_{ij} + \delta_j - \delta_i), \forall i \in N \quad (2)$$

$$Q_i = -|V_i| \sum_{j=1}^N |V_j| \times |Y_{ij}| \times \sin(\theta_{ij} + \delta_j - \delta_i), \forall i \in N \quad (3)$$

178 3.2.2. Technical constraints

179 These are called the inequality restriction and apportioned into:

180 Voltage constraints

$$|V_i^{min}| \leq |V_i| \leq |V_i^{max}|, \forall i \in N \quad (4)$$

181 Current constraints

$$I_{li} \leq I_{li}^{rated}, \forall i \in b \quad (5)$$

182 DG size constraints

$$P_{DG}^{min} \leq P_{DG} \leq P_{DG}^{max} \quad (6)$$

$$Q_{DG}^{min} \leq Q_{DG} \leq Q_{DG}^{max} \quad (7)$$

183 DG location constraints

$$2 \leq DG_{location} \leq N_{bus} \quad (8)$$

184 where L is the energized number of branches; N is the number of buses; Y_{ij} is the bus admittance of
185 line $i-j$; θ_{ij} is the admittance angle of line $i-j$; $|V_i^{min}|$; $|V_i^{max}|$ are the limits of the voltage at the bus
186 i ; I_{li} is the line current flow of line i ; I_{li}^{rated} is the rated line current capacity at line i .

187 3.3. Reliability Assessment for Distribution Systems

188 The measurement of reliability is a crucial agent for the planning and operation of DS. Based on
 189 system configuration and item's reliability data, DS reliability evaluation may forecast the obstruction
 190 of a DS at the client end. The primary goal of reliability analysis is to measure, forecast, and compare
 191 reliability indicators for multiple network topologies for reliability rising. The reliability evaluation
 192 calculates performance at client load points while factoring in the stochastic nature of failures inci-
 193 dence and outage period. The main indicators linked with client points are failure rate (λ), outage time
 194 (r), and yearly unavailability (U), which may be computed using equations (9 - 10).

$$\lambda_p = \sum_{i=1}^N \lambda_i \left(\frac{f}{yr} \right) \quad (9)$$

$$U_p = \sum_{i=1}^N \lambda_i r_i \left(\frac{hr}{yr} \right) \quad (10)$$

$$r_p = \frac{U_p}{\lambda_p} (hr) \quad (11)$$

3.1. Monte-Carlo Simulation Approach

196 Because a power system is uncertain, the Monte-Carlo simulation approach may be used to pro-
 197 vide more exact findings when evaluating its reliability. Monte-Carlo simulation can be classified into
 198 two types: time-sequential and state sampling methods, but the time-sequential technique is utilized
 199 here.

200 State of the basic distribution equipment such as branches, transformers, and protective compo-
 201 nents such as disconnecting switches, breakers, and fuses helps for system reliability valuation. In
 202 general, line segments and transformers may be depicted by two states seen in figure 1, where the
 203 upstate signifies that the portion is operational and the downstate shows that the portion is dud.

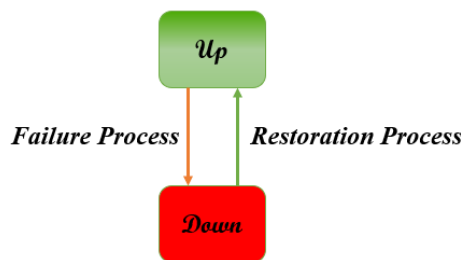


Figure 1. Element state transition diagram

204
 205
 206 The time to failure is the period that the item persists in the upper (TTF) or failure time(FT), But
 207 the period, while an element is down, is called a reconquest time and it might be either the time to
 208 repair(TTR) or the time to substitute. The transition from the up to down is the failure operation,
 209 while the transition from down to up is the restoration operation. Figure 2 depicts the history of simu-
 210 lated element operation and repair.

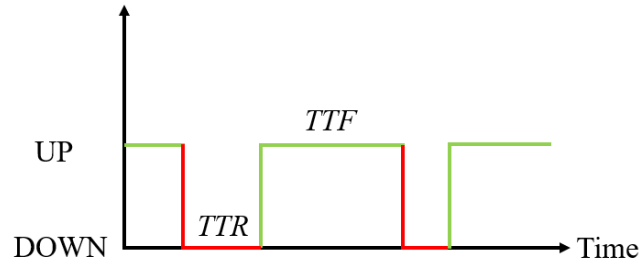


Figure 2. Component Up/Down history

211
212

213 TTF and TTR are randomly generated with potentially varying probabilistic. A universal random
214 number generator can create a uniform distribution direct, and the resulting random numbers are
215 transformed into TTF or TTR using these formulas.

$$TTF = \left(-\log \frac{U}{\lambda} \right) * 8760 \quad (12)$$

$$TTR = -\log U * MTTR \quad (13)$$

216 where U is a haphazard variable in the range $[0, 1]$.

217 3.1. Load Point Failures identification

218 The harshest issue in the emulation is to detect the load points influenced by the fiasco of an el-
219 ement. A complicated RDN can be broken down into primary feeders and laterals. The following is
220 the technique for detecting failing load points and their operation/restoration histories [25]:

221 Discover the failure object and its location, as well as the failed elements number and the lost feeder's
222 amount to which the failed element is linked.

223 Identify the impacted load points that are linked to the failing feeder, as well as their failure intervals,
224 based on the setup and protection system of the damaged feeder.

225 Determine the downstream feeders linked to the damaged feeder's sub-feeders and the impact of the
226 damaged component on the load points linked to these sub-feeders.

227 Repeat steps 2 and 3 for every failing sub-feeder till all sub-feeders linked to the failing feeder are
228 identified and analyzed.

229 Find the upstream feeder to which the failing feeder is linked, as well as the impacts of the failure
230 component on the load points in the upstream feeder.

231 Reiterate (2) to (5) until the primary feeder is reached and assessed.

232 The client obstruction indicators will be used to quantify system reliability; the main indicators are the
233 customer average interruption duration index (CAIDI), the system average interruption frequency
234 index (SAIFI), the system average interruption duration index (SAIDI), the average service availabil-
235 ity index (ASAI), and the energy not supplied index (ENS). The following equations are used to com-
236 pute them [26]:

$$SAIFI = \frac{\sum_{i=1}^k \lambda_i N_i}{\sum_{i=1}^k N_i} \quad (14)$$

$$SAIDI = \frac{\sum_{i=1}^k U_i N_i}{\sum_{i=1}^k N_i} \quad (15)$$

$$CAIDI = \frac{\sum_{i=1}^k U_i N_i}{\sum_{i=1}^k \lambda_i N_i} = \frac{SAIDI}{SAIFI} \quad (16)$$

$$ASAI = \frac{\sum_{i=1}^k 8760 N_i - \sum_{i=1}^k U_i N_i}{\sum_{i=1}^k 8760 N_i} \quad (17)$$

$$ENS = \sum_{i=1}^k U_i L_i \quad (18)$$

237 where U_i is the annual outage time, N_i is the number of customers at load point i , λ_i is the failure rate,
 238 and " L_i " is the average load connected to load point i and 8760 is the number of hours in a calendar
 239 year.

240 The developed flow chart of the computer program to determine the distribution system reliabil-
 241 ity indices consists of the following steps:

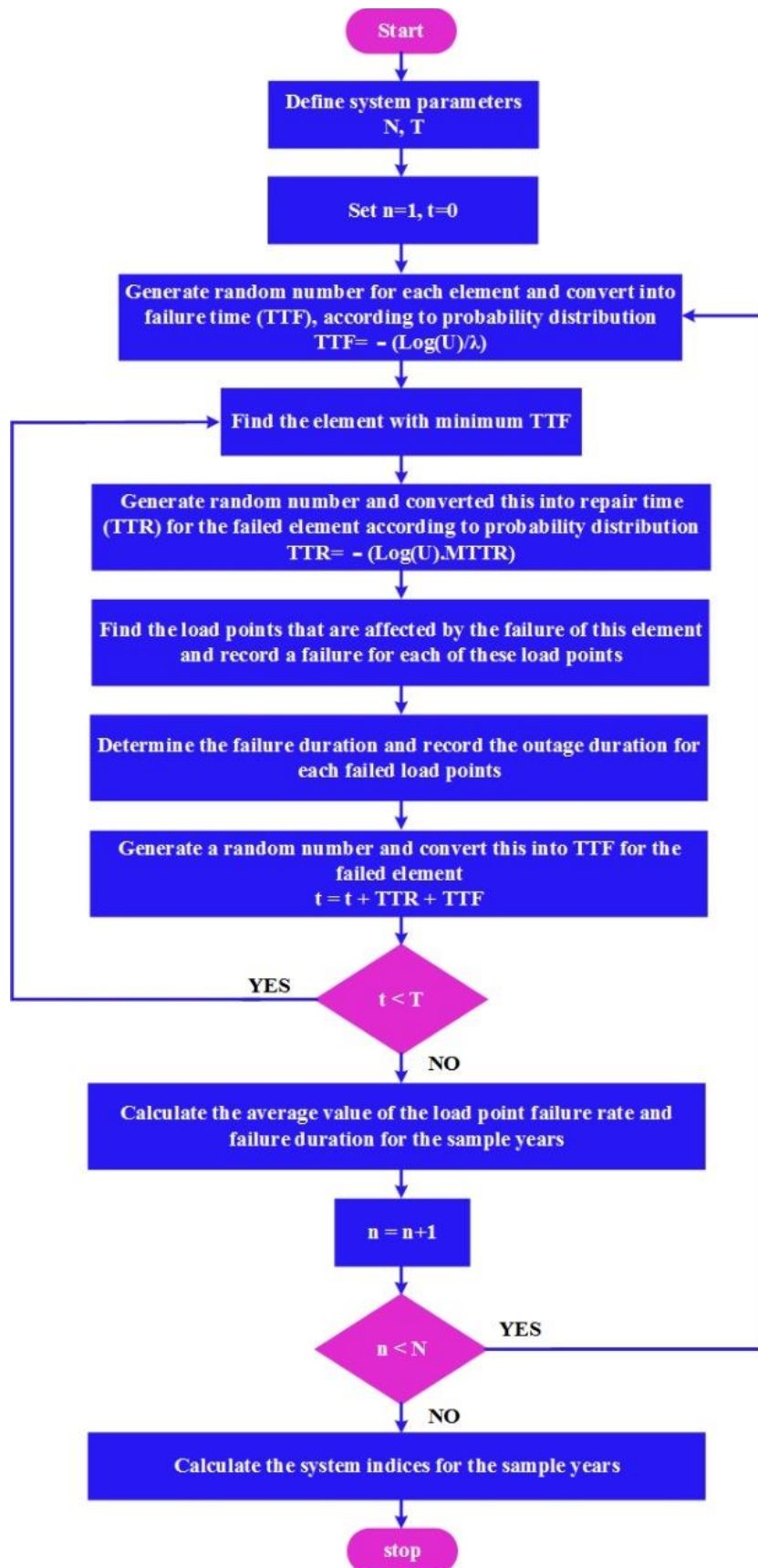


Figure 3. Flowchart for Monte Carlo Simulation

245 4. Mathematical Model of Optimization Techniques

246 4.1. Wild horse optimizer (WHO)

247 For addressing optimization issues, the wild horse optimizer (WHO) technique mathematically
248 simulates and duplicates the social life behavior of these wild horses in nature. [27]. Horses predomi-
249 nately live in herds with a stallion and many foals and mares. They exhibit a variety of behaviors,
250 including mating and grazing, pursuing, dominating, commanding. Five steps for the WHO algorithm
251 are listed below:

252 4.1.1. Generating an initial population and formation horse groups and choosing leaders

253 First, the initial population is divided into numerous groups. N is the number of the population
254 and G is the number of groups in the algorithm. Each group has a leader (stallion), so the number of
255 stallions in the algorithm equals G, and (N-G) is the remaining population (Foals and mares) are dis-
256 tributed similarly among these groups. Figure 4 presents how the stallions and foals have been chosen
257 from the initial population to produce various groups.

258 4.1.2. Grazing behavior

259 The following equation was proposed to simulate the grazing behavior:

$$X_{i,G}^j = 2Z \cos(2\pi RZ) \times (Stallion^j - X_{i,G}^j) + Stallion^j \quad (19)$$

260 where $X_{i,G}^j$ denotes the current location of the foal or mare group member, $Stallion^j$ is the stallion posi-
261 tion, R is a uniform stochastic number from the range [-2,2], and Z is the adaptive mechanism calcu-
262 lated from the following equation:

$$P = \overline{R}_1 < TDR; \quad IDX = (P == 0); \quad Z = R_2 \theta IDX + \overline{R}_3 \theta (\sim IDX) \quad (20)$$

263 where P is a vector consisting of 0 to 1, \overline{R}_1 and \overline{R}_3 are a random number from the range [0,1], R_2 is a
264 uniform random number from the range [0,1]. TDR is an adaptive parameter that starts with 1 and
265 decreases until it reaches 0 at the end of the implementation of the algorithm according to the follow-
266 ing equation:

$$TDR = 1 - it \times \left(\frac{1}{maxit}\right) \quad (21)$$

267 where *it* is the current iteration and *maxit* is the maximum number of iterations.

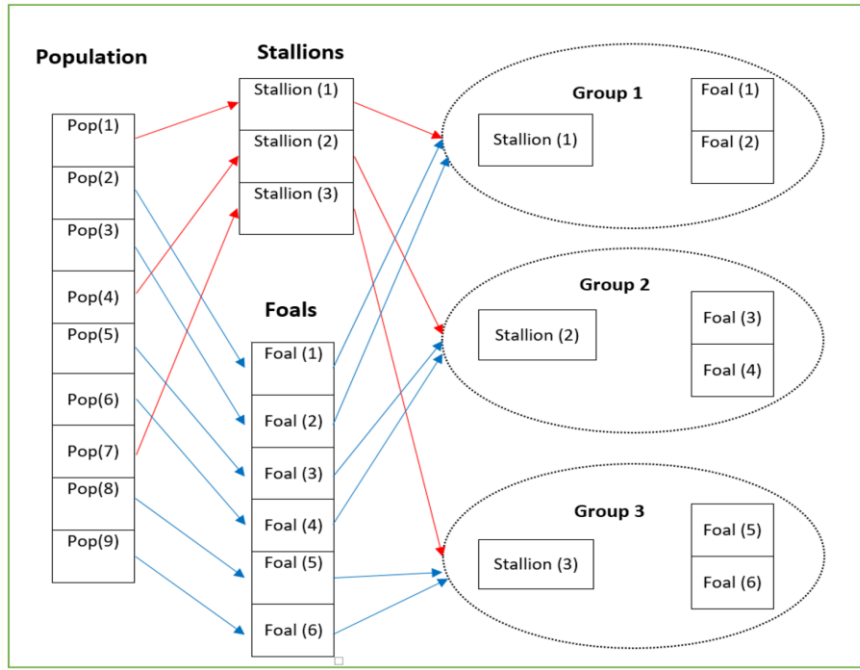


Figure 4. Formation of groups from the original population.

268

269

270

271 4.1.3. Horse mating behavior

272 To implement the mating behavior of horses, a foal goes from group i to a temporary group while
 273 a foal goes from group j to a temporary group. To simulate the mating behavior of horses, the Crossover
 274 ver operator of the mean type was proposed as follows:

$$X_{G,K}^p = Crossover(X_{G,i}^q, X_{G,j}^z) \quad i \neq j \neq k, p = q = end, Crossover = Mean \quad (22)$$

275 4.1.4. Group leadership

276 In the WHO algorithm, the Stallions (group leaders) lead the group to the water hole. The Stallions
 277 lions compete for this water hole so that the domination group can employ this water hole firstly and
 278 then other groups can use the water hole. The following equation was recommended for this step of
 279 the algorithm:

$$\overline{Stallion}_{G_i} = \begin{cases} 2Z \cos(2\pi RZ) \times (WH - Stallion_{G_i}) + WH & \text{if } R_3 > 0.5 \\ 2Z \cos(2\pi RZ) \times (WH - Stallion_{G_i}) - WH & \text{if } R_3 \leq 0.5 \end{cases} \quad (23)$$

280 where $\overline{Stallion}_{G_i}$ is the next position of the leader. WH is the location of the water hole.

281

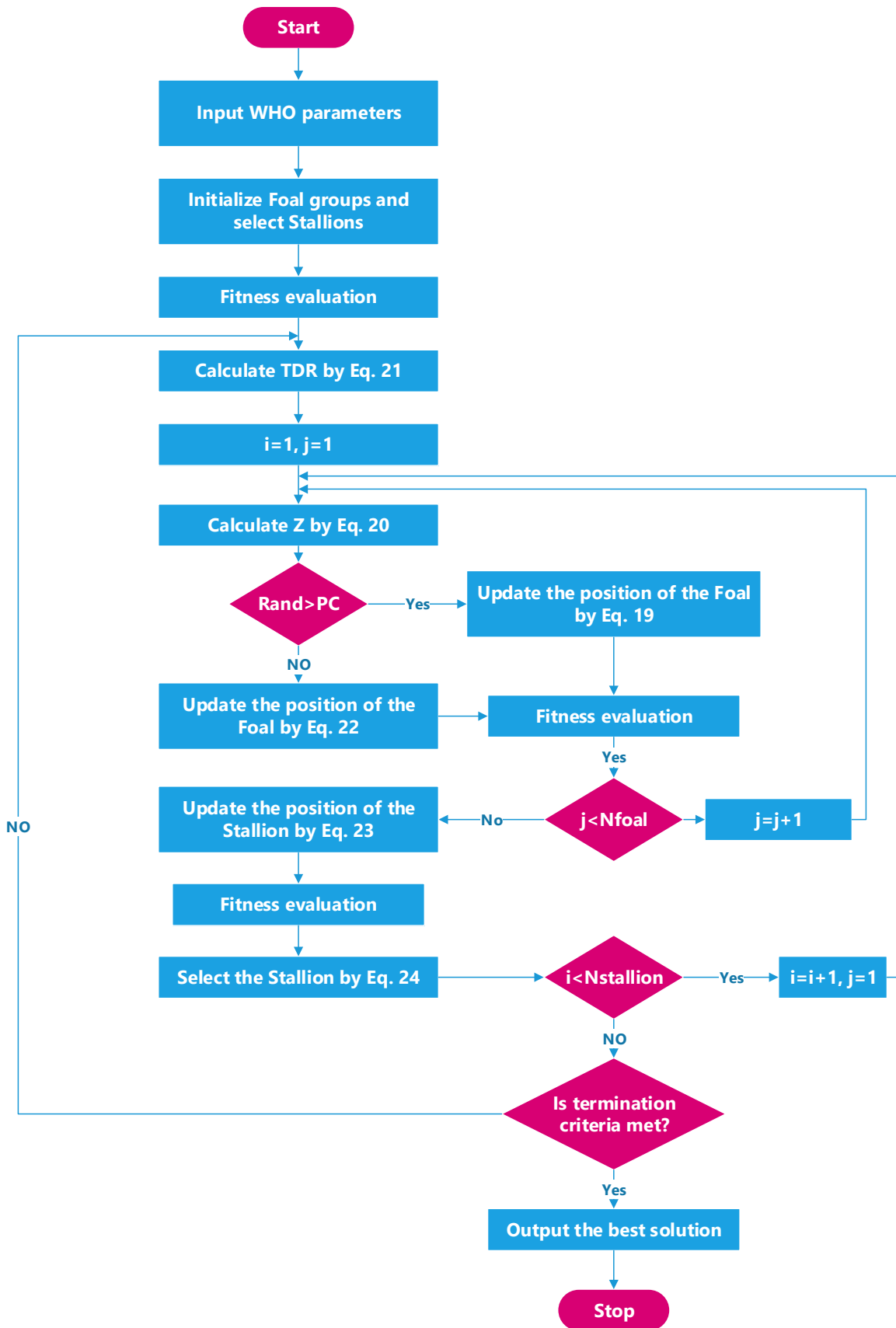
282 4.1.5. Leaders interchange and selection

283 In the following stages, leaders are chosen according to fitness. The leader position and the relevant
 284 member will change based on this equation:

$$\overline{Stallion}_{G_i} = \begin{cases} X_{G,i} & \text{if } \text{cost}(X_{G,i}) < \text{cost}(Stallion_{G_i}) \\ Stallion_{G_i} & \text{if } \text{cost}(X_{G,i}) > \text{cost}(Stallion_{G_i}) \end{cases} \quad (24)$$

285

Fig. 5 presents the flow chart of WHO algorithm.



286

287

Figure 5. The flow chart of WHO algorithm.

288

289 4.2. Improved Wild horse optimizer (IWHO)

290 The Improved Wild horse optimizer (IWHO) is based on the cuckoo search (CS) algorithm [28].
 291 During the iteration of the proposed algorithm, the new solution is generated using the Levy flight as
 292 the following equation:

$$X_{i,G} = X_{i,G} - \gamma(X_{i,G} - X_g) \oplus Levy(\lambda) = X_{i,G} + \frac{0.01u}{|v|^{1/\lambda}}(X_{i,G} - X_g) \quad (25)$$

293 where $X_{i,G}$ is the i -th position of the group member, γ denotes the step scaling size, X_g denotes the
 294 global best solution, the \oplus refers to the process of element-wise multiplications, λ refers to the Levy
 295 flight exponent, while u and v are defined as:

$$u \sim N(0, \sigma_u^2) \quad , \quad v \sim N(0, \sigma_v^2) \quad (26)$$

296 The standard deviations σ_u and σ_v are expressed as:

$$\sigma_u = \left[\frac{\sin\left(\frac{\lambda\pi}{2}\right) \cdot \Gamma(1 + \lambda)}{2^{(\lambda-1)} \lambda \cdot \Gamma\left(\frac{1 + \lambda}{2}\right)} \right]^{1/\lambda} \quad , \quad \sigma_v = 1 \quad (27)$$

297 where Γ is the Gamma function, then, the new candidate solution is generated, the eq. 21 is applied.
 298 The principal advantage of this improvement is the ability of the proposed technique to balance global
 299 exploration and local exploitation [29]. Figure 6 shows the flow chart of IWHO algorithm.

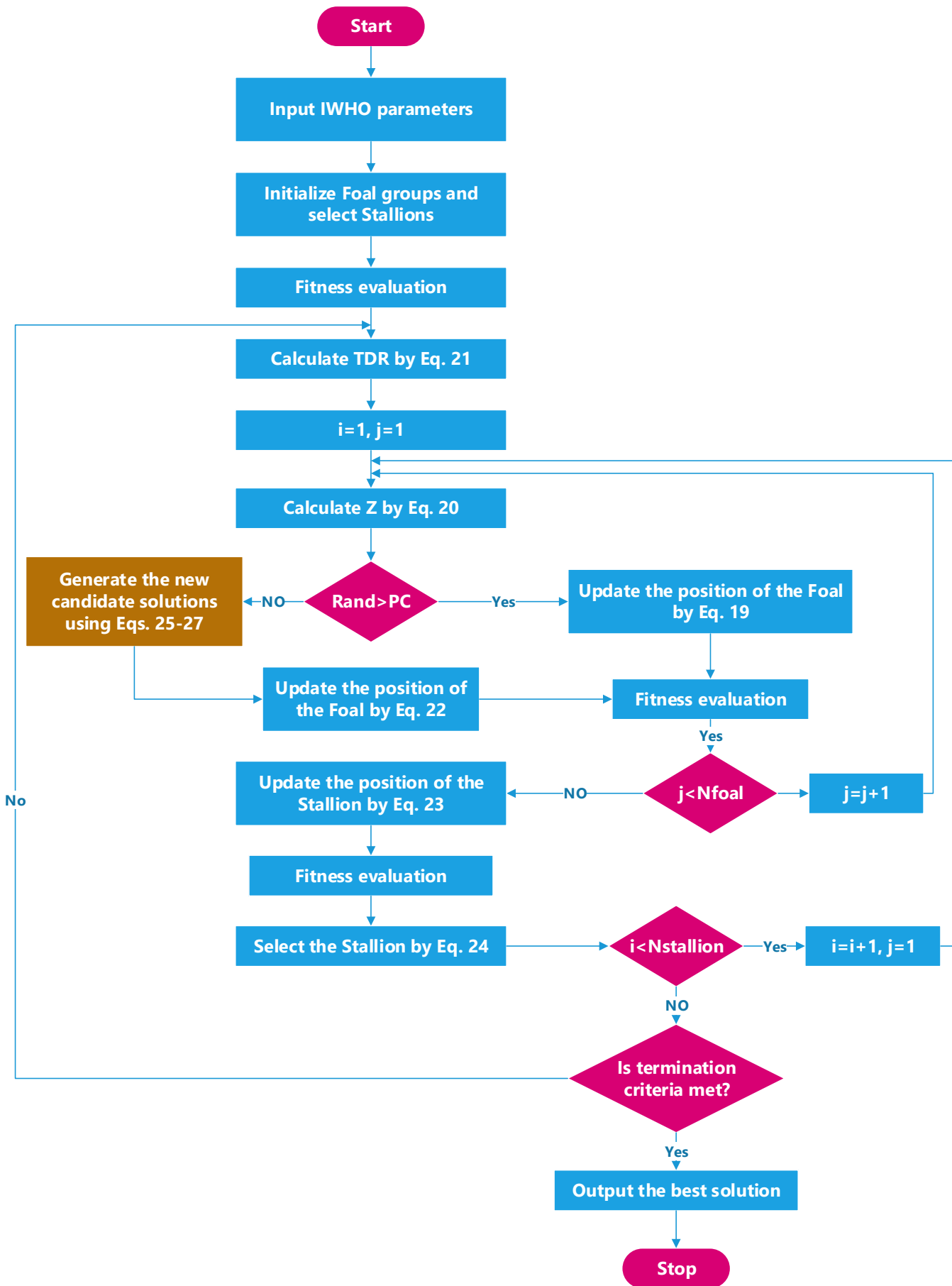


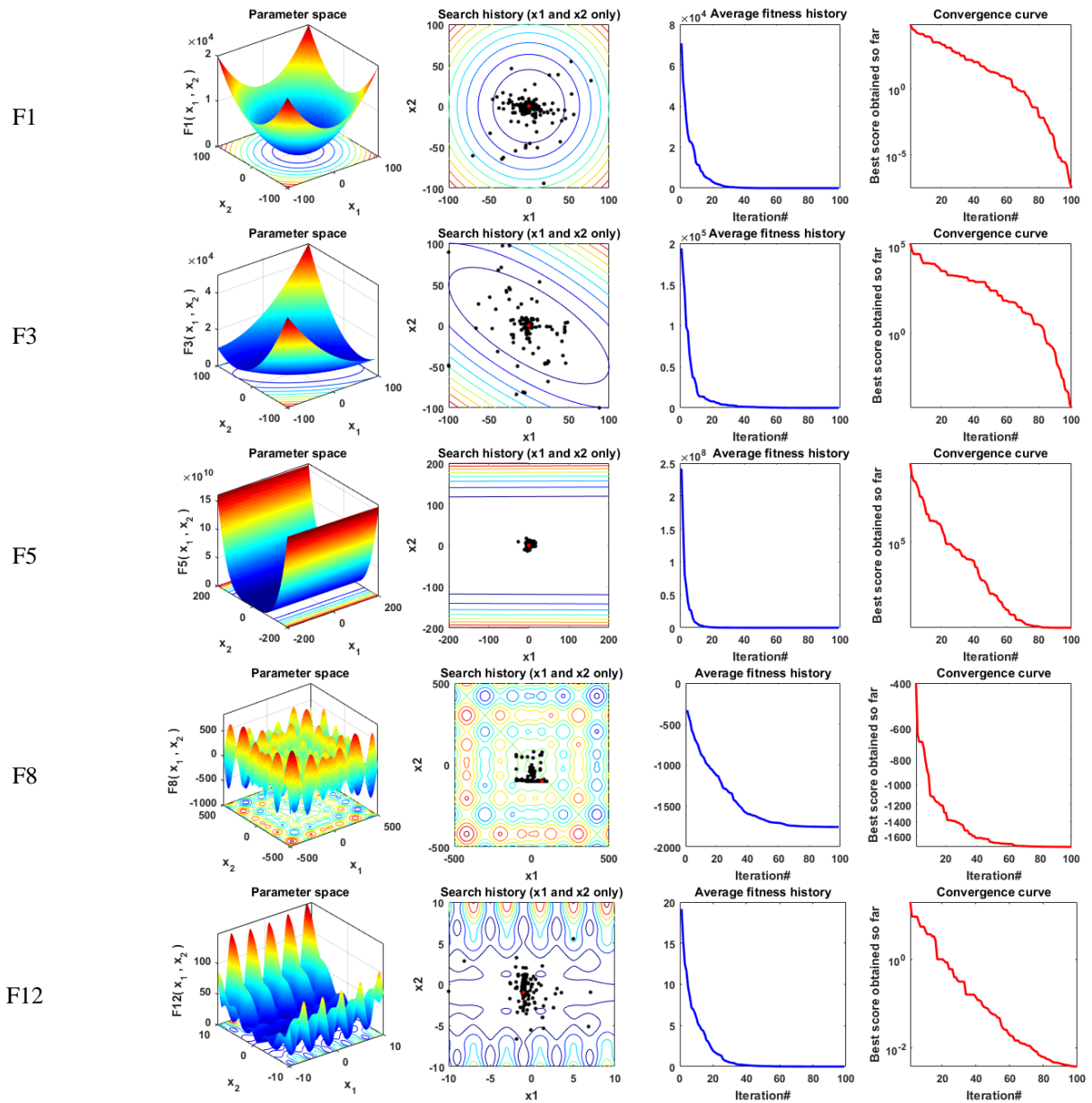
Figure 6. The flow chart of IWHO algorithm.

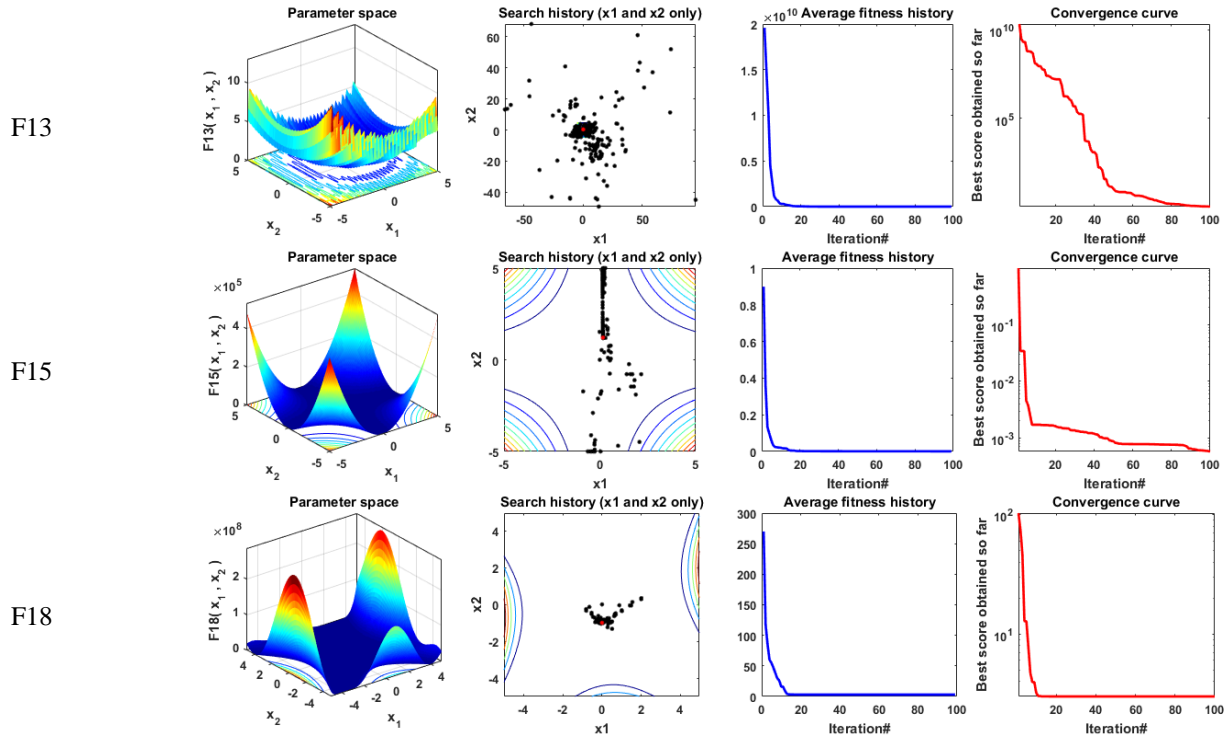
302 **5. Simulation Results and Discussion**

303 *5.1. Mathematical validation*

304 To evaluate the robustness of the suggested IWHO algorithm, it was run separately on all 23 OFs
 305 for the maximum iterations number of 1000 and the agents' number of 50. To assess the algorithm's
 306 performance, this research uses both quantitative and qualitative measures. Fig.7 shows the qualitative
 307 metrics for some the benchmark functions, including 2D views of the functions, search histories,
 308 mean fitness histories, and convergence curves.

309





310 **Figure 7.** Qualitative metrics on some benchmark functions: 2D views of the functions, search history, mean fitness history,
 311 and convergence characteristics curve.

312 Also, the suggested IWHO was tested for its ability to provide a quasi-suitable solution on a col-
 313 lection of 23 objective functions of various types of unimodal, multi-modal, and fixed-dimensional
 314 composite functions [30]. The obtained results are compared with three recent algorithms Grey Wolf
 315 Optimizer (GWO) algorithm [31], Tunicate Swarm Algorithm (TSA) [32], and Seagull Optimization
 316 Algorithm (SOA) [33], as well as the original WHO. The parameter setting of the chosen algorithms
 317 is shown in table 1. Each optimisation technique was executed in 20 independent runs; the optimiza-
 318 tion results are presented as the best, worst, average, and the standard deviation (std) of the preferable
 319 solutions, respectively.

320 **Table 1.** Parameter sets of the chosen algorithms.

Algorithms	Parameters setting
Common settings	Population size: nPop=50 Maximum iterations : Max_iter=1000 Number of separate runs: 20
SOA	b=1
IWHO	PS=0.2; % Stallions Percentage
WHO	PC=0.13; % Crossover Percentage

321

322 5.1.1. Evaluation of the Objective Functions Findings for Unimodal

323 The suggested algorithm's exploitative capacity may be assessed and evaluated using the uni-
 324 modal test functions. Table 1 displays the best values achieved using the proposed and well-known
 325 optimization algorithms for these benchmark functions. It can be noticed that the IWHO technique

326 provides better results on all unimodal functions except F7 which the original WHO reaches only for
 327 the best answer while the proposed algorithm achieves the best values for it in the worst, mean, and
 328 std. The suggested IWHO method produces better results than existing approaches for all unimodal
 329 test functions. Figure 8 depicts the convergence characteristics curves of the introduced IWHO ap-
 330 proach, including well optimization techniques for unimodal benchmark functions. For more analysis
 331 to confirm the performance of the recommended technique, a boxplot of outcomes for each technique
 332 and OF is demonstrated in Figure 9.

333

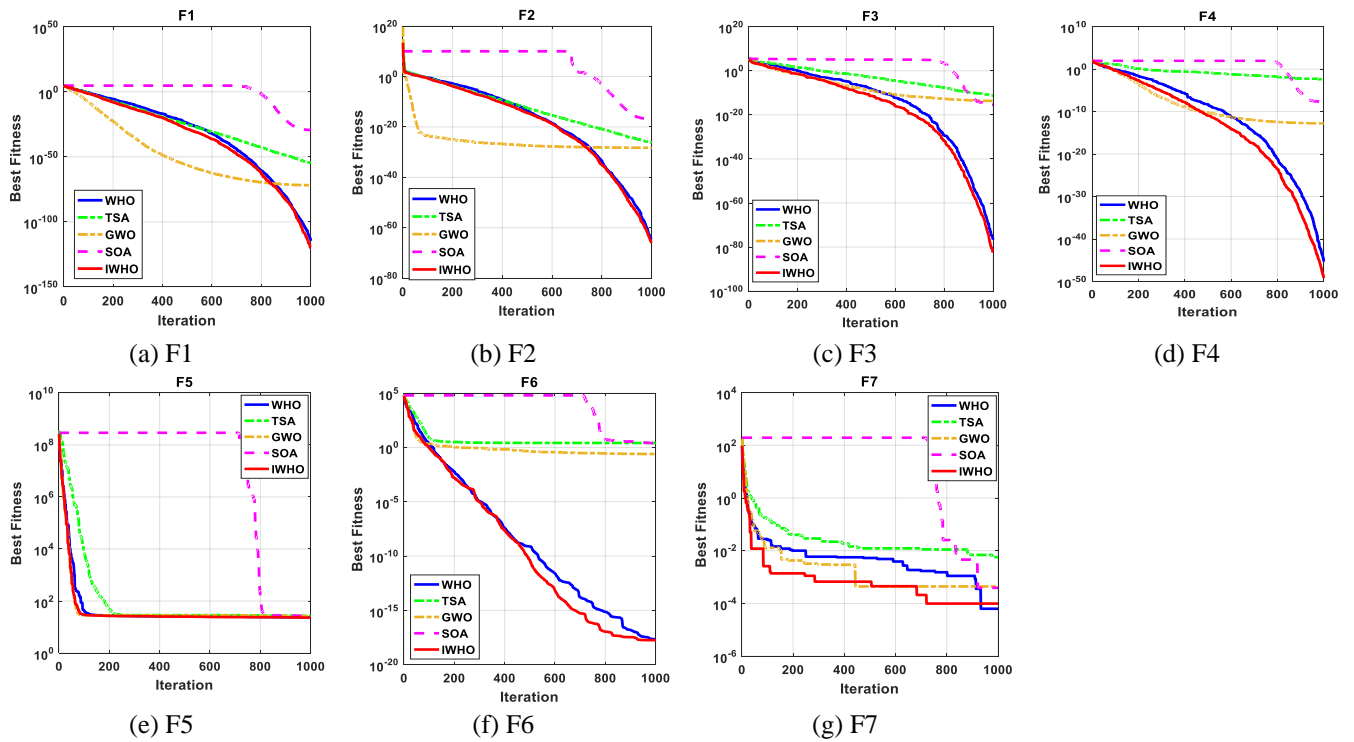
334

Table 2. Benchmark function outcomes for unimodal.

Function		WHO	IWHO	GWO	TSA	SOA
F1	Best	2.6E-115	8.2E-121	1.6E-72	2.82E-55	4.76E-30
	Worst	9.5E-106	1.4E-108	3.42E-07	3.45E-17	5.06E-10
	Mean	1.1E-106	6.9E-110	1.71E-08	1.72E-18	2.53E-11
	std	2.8E-106	3.1E-109	7.65E-08	7.71E-18	1.13E-10
F2	Best	1.53E-65	1.18E-66	5.52E-29	6.19E-27	1.3E-17
	Worst	1.03E-59	2.14E-61	4.4E-08	7.35E-13	4.26E-08
	Mean	2E-60	1.49E-62	2.39E-09	3.68E-14	2.15E-09
	std	3.17E-60	4.81E-62	9.81E-09	1.64E-13	9.52E-09
F3	Best	1.95E-77	3.99E-83	2.22E-14	6.22E-12	4.12E-16
	Worst	6.75E-64	3.47E-68	1.200307	195.9186	0.54897
	Mean	4.99E-65	1.75E-69	0.175247	24.31458	0.039322
	std	1.63E-64	7.76E-69	0.401434	60.03018	0.124825
F4	Best	4.83E-46	6.5E-50	1.7E-13	0.004211	1.88E-08
	Worst	4.2E-41	1.16E-42	0.123216	21.22892	1.489819
	Mean	4.68E-42	7.93E-44	0.012534	3.538218	0.21736
	std	1.18E-41	2.63E-43	0.037861	6.441649	0.523316
F5	Best	23.62242	23.06539	26.41102	27.10919	27.20026
	Worst	28.53885	24.57677	28.93196	28.92147	28.93044
	Mean	24.46879	24.07834	27.85099	28.38438	28.54089
	std	1.000308	0.415118	0.799818	0.675004	0.57121
F6	Best	2.19E-18	1.78E-18	0.249992	2.596274	2.507228
	Worst	2.92E-14	2.84E-15	6.754946	6.30706	6.133702
	Mean	2.04E-15	4.52E-16	2.39919	4.176579	4.253747
	std	6.58E-15	7.79E-16	1.752866	1.013975	1.034333
F7	Best	6.26E-05	9.83E-05	0.000439	0.005675	0.000389
	Worst	0.00123	0.00078	0.008863	0.052199	0.024776
	Mean	0.000421	0.000293	0.00327	0.014535	0.006081
	std	0.00027	0.000162	0.002825	0.010611	0.006765

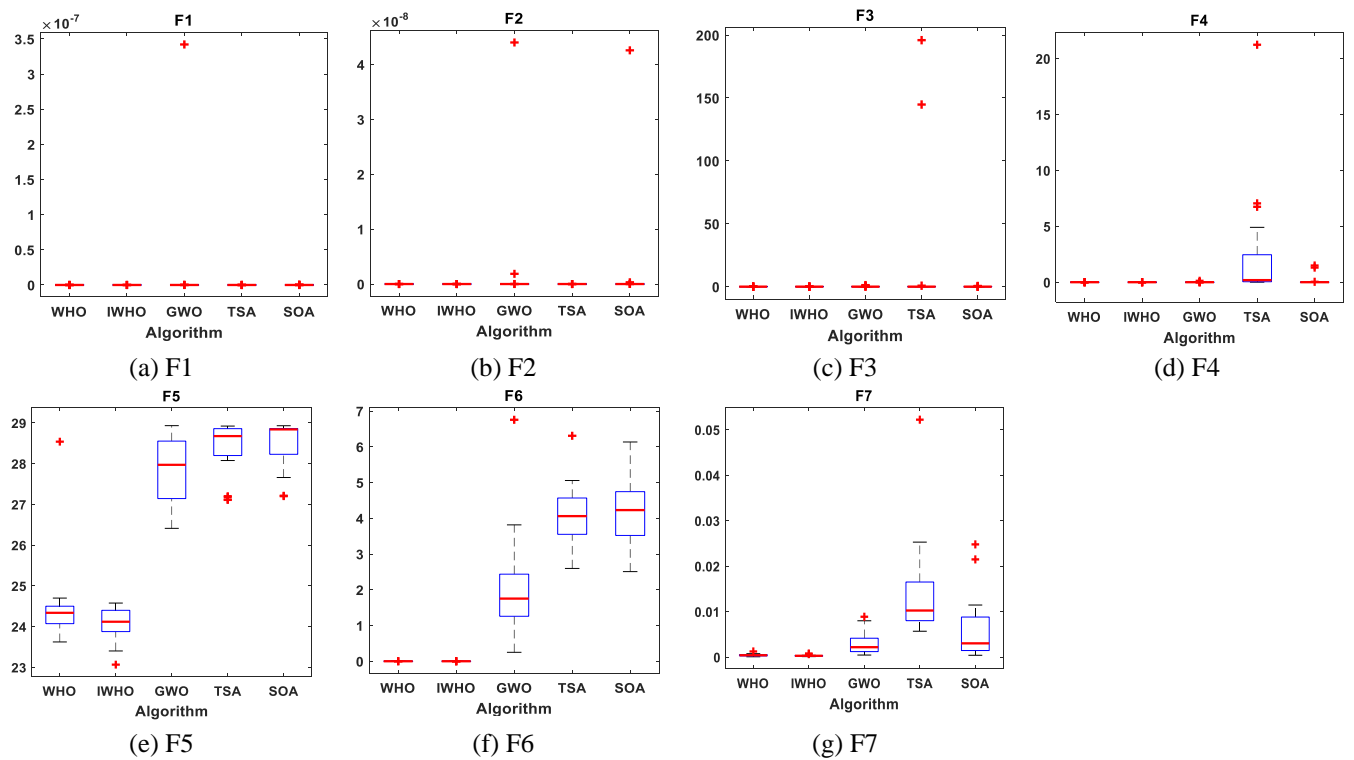
The best values obtained are in bold

335



336

Figure 8. The convergence curves of all algorithms for unimodal benchmark functions.



337

Figure 9. Boxplots for all algorithms for unimodal benchmark functions.

338 5.1.2. Evaluation of the Objective Functions Findings for multi-modal

339 Six objective functions of multi-modal functions, including F8 to F13, were chosen to evaluate
 340 the performance of the proposed IWHO technique in presenting the best solutions. The results of the
 341 implementation of the IWHO algorithm and three other optimization algorithms as well as the con-

342 ventional WHO algorithm on this type of objective function, are displayed in Table 2. The emulation
 343 results prove that the IWHO performs better and more competitively in tackling this sort of optimiza-
 344 tion issue. Fig. 10 displays the convergence curves of IWHO and other rival methods. Fig. 11 presents
 345 the box plot for the proposed IWHO and other concurrent algorithms on multi-modal functions. Ac-
 346 cording to the results, the proposed IWHO technique is the greatest optimization technique for the
 347 majority of the evaluation metrics.

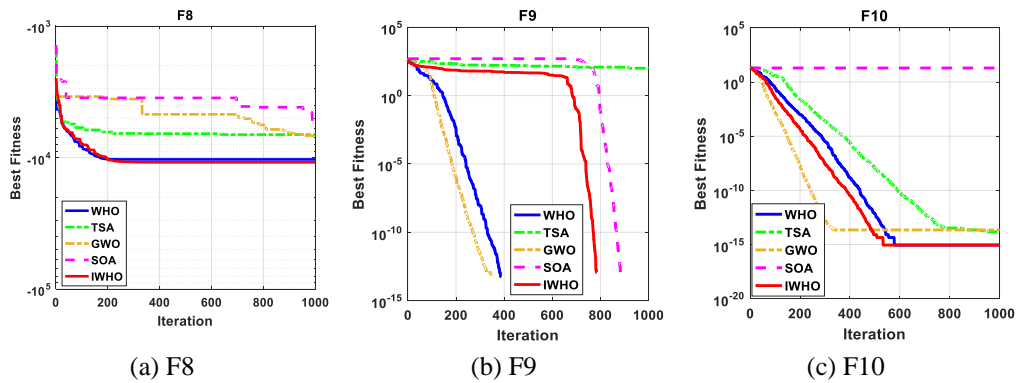
348

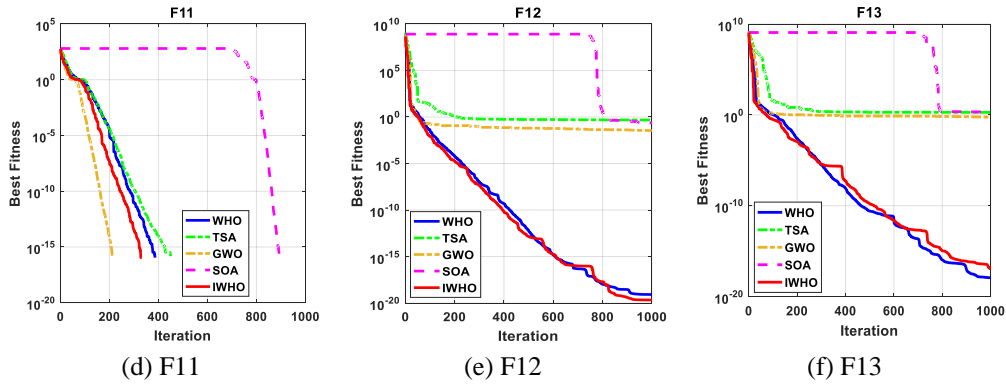
Table 3. Benchmark function outcomes for multi-modal.

Function		WHO	IWHO	GWO	TSA	SOA
F8	Best	-10331.3	-10867.3	-6876.85	-6687.08	-5688.53
	Worst	-8811.26	-8909.96	-2040.64	-3353.87	-3025.17
	Mean	-9512.65	-9654.44	-5363.86	-5404.01	-4662.31
	std	377.1542	469.3701	1298.089	964.0392	721.2641
F9	Best	0.00E+00	0.00E+00	0.00E+00	101.0783	0.00E+00
	Worst	0.00E+00	0.00E+00	10.64299	312.5106	19.6612
	Mean	0.00E+00	0.00E+00	1.088214	196.4102	2.489027
	std	0.00E+00	0.00E+00	2.989658	51.77915	5.370562
F10	Best	8.88E-16	8.88E-16	2.22E-14	1.51E-14	19.95954
	Worst	4.44E-15	4.44E-15	4.94E-07	2.891204	19.96677
	Mean	3.2E-15	3.02E-15	2.56E-08	0.545612	19.96242
	std	1.74E-15	1.79E-15	1.1E-07	1.123192	0.001919
F11	Best	0.00E+00	0.00E+00	0.00E+00	0.00E+00	0.00E+00
	Worst	0.00E+00	0.00E+00	0.034439	0.151418	0.11477
	Mean	0.00E+00	0.00E+00	0.003728	0.029085	0.013796
	std	0.00E+00	0.00E+00	0.009503	0.052147	0.033163
F12	Best	8.23E-20	2.12E-20	0.035117	0.478781	0.237936
	Worst	0.103669	0.207317	1.373427	18.46794	1.633411
	Mean	0.010367	0.020732	0.253217	6.960091	0.619033
	std	0.031909	0.063811	0.394467	5.091209	0.411038
F13	Best	1.2E-18	1.1E-17	0.569956	1.889159	1.854413
	Worst	0.109867	0.175786	2.764004	3.467599	2.898385
	Mean	0.019212	0.034458	1.354047	2.824032	2.29935
	std	0.028468	0.050856	0.672746	0.437644	0.298225

The best values obtained are in bold

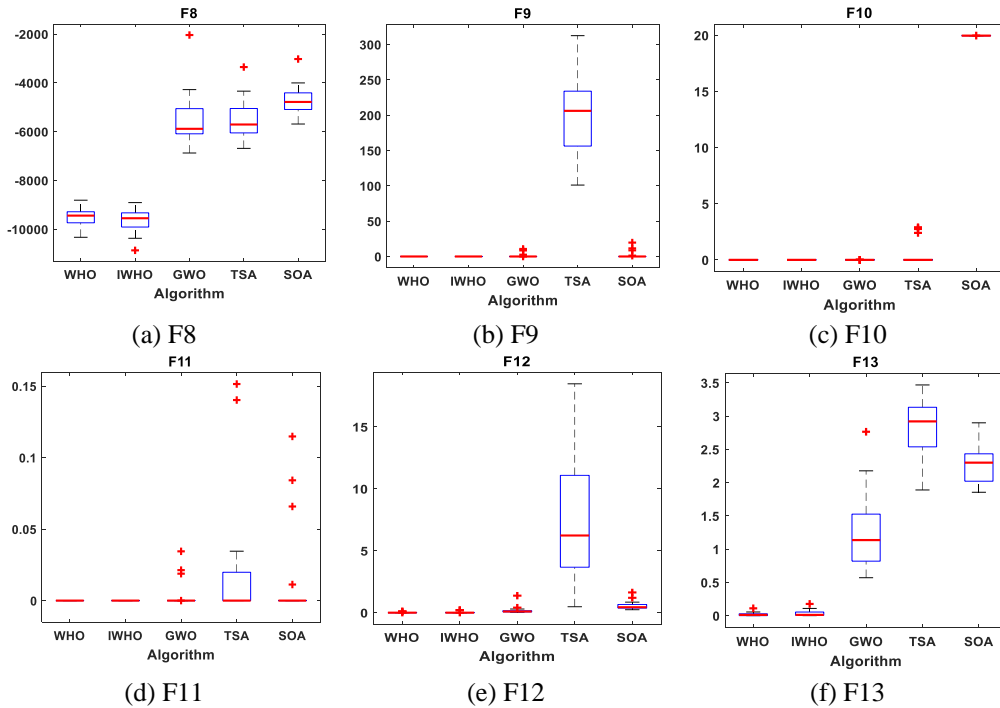
349





350

Figure 10. The convergence curves of all algorithms for multi-modal benchmark functions.



351

Figure 11. Boxplots for all algorithms for multi-modal benchmark functions.

352 5.1.3. Evaluation Results on composite Objective Functions

353 Ten objective functions of composite functions, including F14 to F23, were chosen to assess the
 354 performance of the proposed IWHO in providing optimal solutions. Table 3 presents the best opti-
 355 mum solutions found by all algorithms, including the best, worst, average, and STD. Fig. 12 displays
 356 the convergence curves of the proposed IWHO technique and other techniques achieved in the multi-
 357 ple benchmark functions. Fig. 13 displays the boxplots for F14 to F23. It can be seen that the boxplots
 358 of the proposed IWHO when compared to other techniques, are highly tight for the majority of these
 359 functions with the lowest values.

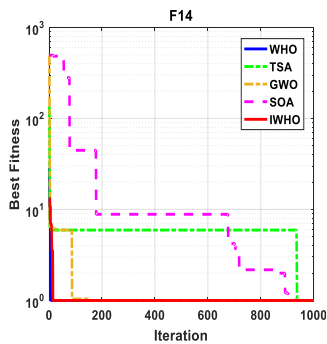
360

Table 4. Results of composite benchmark functions.

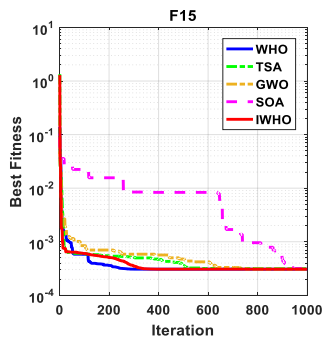
Function		WHO	IWHO	GWO	TSA	SOA
F14	Best	0.998004	0.998004	0.998004	0.998004	0.998004
	Worst	5.928845	2.982105	12.67051	12.67051	12.67051
	Mean	1.294247	1.14691	5.686485	7.493557	4.423671

	std	1.113224	0.485651	4.930301	4.617822	4.324715
	Best	0.000307	0.000307	0.000308	0.000314	0.000312
F15	Worst	0.020363	0.001223	0.120459	0.088541	0.00143
	Mean	0.001485	0.000399	0.007588	0.010089	0.001171
	std	0.004459	0.000282	0.026933	0.020407	0.000273
	Best	-1.03163	-1.03163	-1.03163	-1.03163	-1.03163
F16	Worst	-1.03163	-1.03163	-0.99999	-0.99999	-1.00018
	Mean	-1.03163	-1.03163	-1.03002	-1.0253	-1.03005
	std	1.25E-16	1.76E-16	0.007069	0.012979	0.007032
	Best	0.397887	0.397887	0.397887	0.397887	0.397889
F17	Worst	0.397887	0.397887	0.39789	0.397983	0.398107
	Mean	0.397887	0.397887	0.397888	0.397908	0.397927
	std	0.00E+00	0.00E+00	5.33E-07	2.77E-05	5.14E-05
	Best	3	3	3	3	3
F18	Worst	3	3	3.000023	30.00016	3.000026
	Mean	3	3	3.000004	8.400019	3.000003
	std	6.28E-16	4.78E-16	5.43E-06	11.0806	5.99E-06
	Best	-3.86278	-3.86278	-3.86278	-3.86278	-3.86262
F19	Worst	-3.86278	-3.86278	-3.8549	-3.86269	-3.85477
	Mean	-3.86278	-3.86278	-3.86173	-3.86275	-3.85527
	std	2.28E-15	2.28E-15	0.002504	2.27E-05	0.001731
	Best	-3.322	-3.322	-3.32199	-3.3214	-3.13591
F20	Worst	-3.2031	-3.2031	-3.13491	-2.43163	-2.06108
	Mean	-3.26255	-3.26849	-3.24315	-3.19273	-3.00309
	std	0.060991	0.060685	0.077104	0.197413	0.227568
	Best	-10.1532	-10.1532	-10.1532	-10.1119	-10.1351
F21	Worst	-2.68286	-2.63047	-5.05519	-2.61588	-0.35065
	Mean	-8.89864	-9.14865	-9.64539	-7.14247	-4.32683
	std	2.632293	2.494251	1.562102	3.341539	4.57182
	Best	-10.4029	-10.4029	-10.4029	-10.3678	-10.4004
F22	Worst	-10.4029	-2.7659	-10.4023	-2.70045	-0.90807
	Mean	-10.4029	-9.42345	-10.4026	-8.34157	-7.69481
	std	2.61E-15	2.423101	0.000173	3.074106	3.963887
	Best	-10.5364	-10.5364	-10.5363	-10.4781	-10.5232
F23	Worst	-2.87114	-2.87114	-10.5358	-2.41561	-0.94448
	Mean	-9.8181	-9.38662	-10.5361	-8.56594	-7.46184
	std	2.216446	2.808152	0.000159	3.314441	3.716296

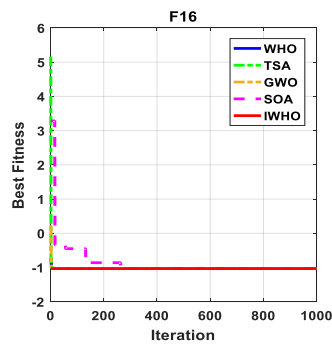
The best values obtained are in bold



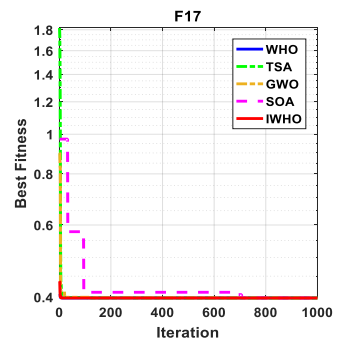
(a) F14



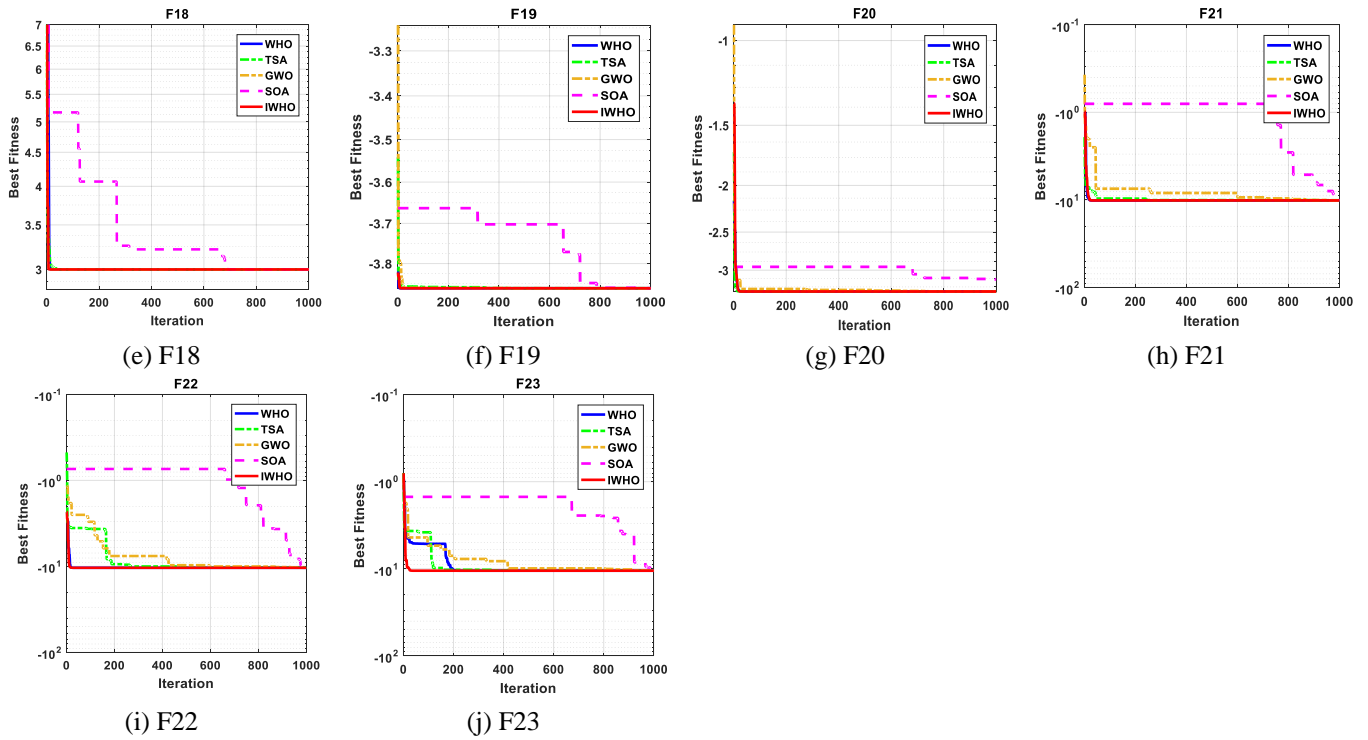
(b) F15



(c) F16

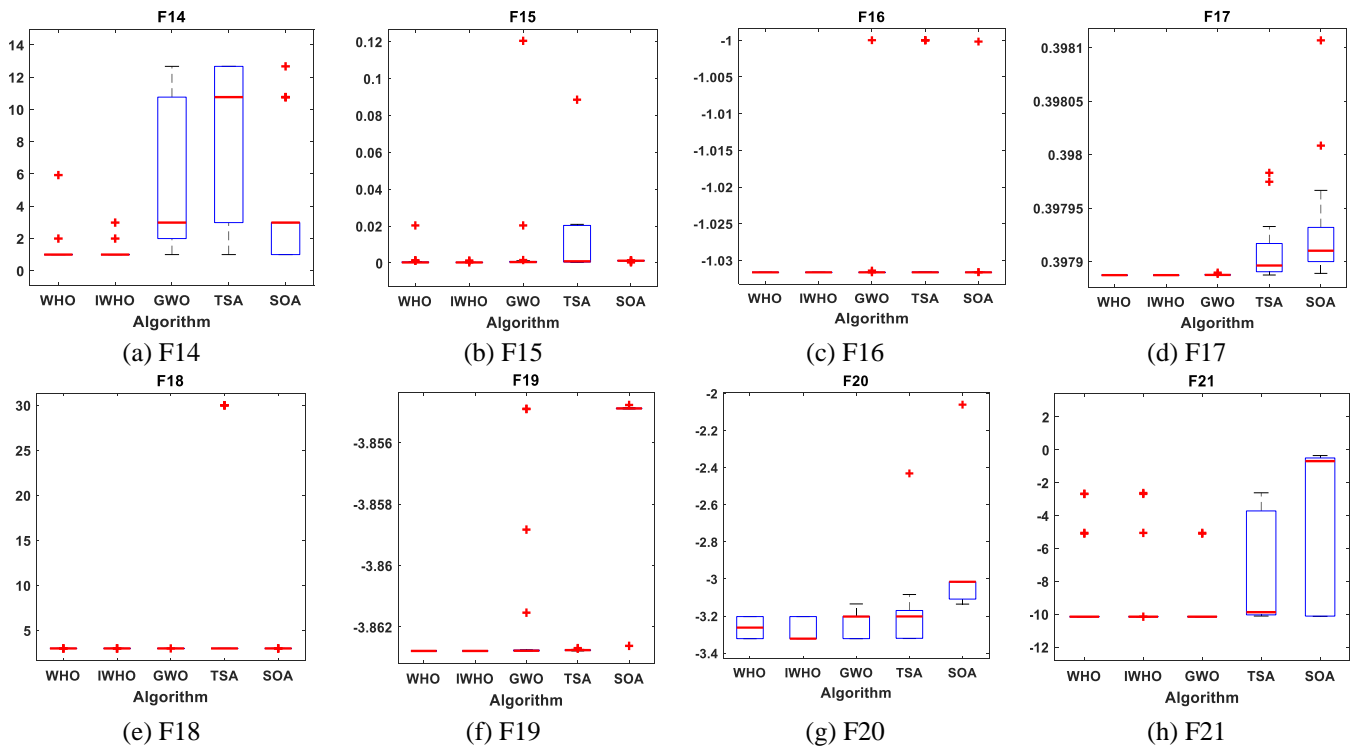


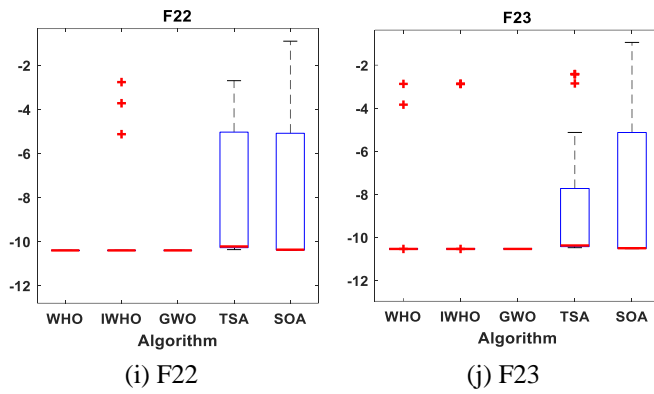
(d) F17



361

Figure 12. The convergence curves of all algorithms for composite benchmark functions.





362 **Figure 13.** Boxplots for all algorithms for composite benchmark functions.

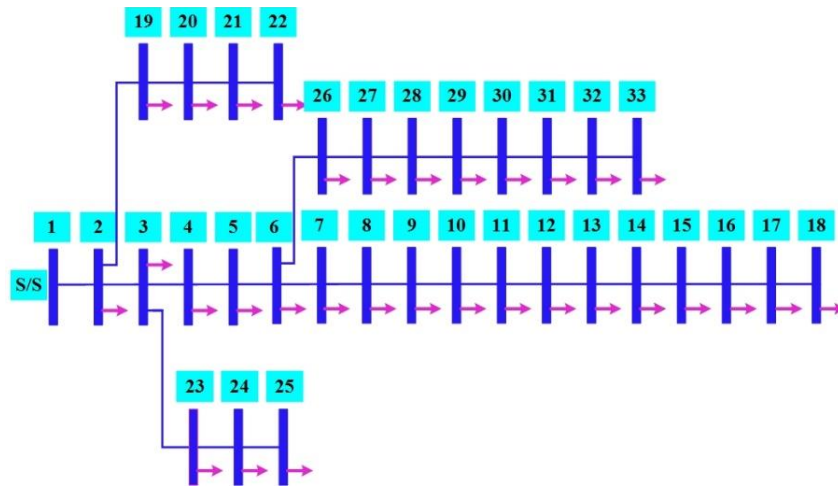
363 **5.2. Test Systems**

364 The described algorithm was employed and validated on IEEE 33 and 69-bus networks to ensure
 365 its usefulness. The starting node voltage is assumed to be 1pu, and all loading buses are considered
 366 viable installation options. MATLAB 2020b software was used to perform the suggested technique
 367 utilizing Intel(R) Core(TM) i7-8550U CPU @ 1.80GHz 1.99 GHz, 16 GB RAM, 64-bit operation
 368 system.

369 **Table 5.** The algorithm parameters and operative restrictions

Parameters	Value
Number of Population	30
Maximum iteration numbers	100
Stallions Percentage	0.2
Crossover Percentage	0.13
Base MVA	100 MVA
Base kV	12.66 kV
Node system voltage constraints	$0.9pu \leq V_i \leq 1.1pu$
DG's power generation constraints	$0MW \leq P_{DG} \leq 3MW$

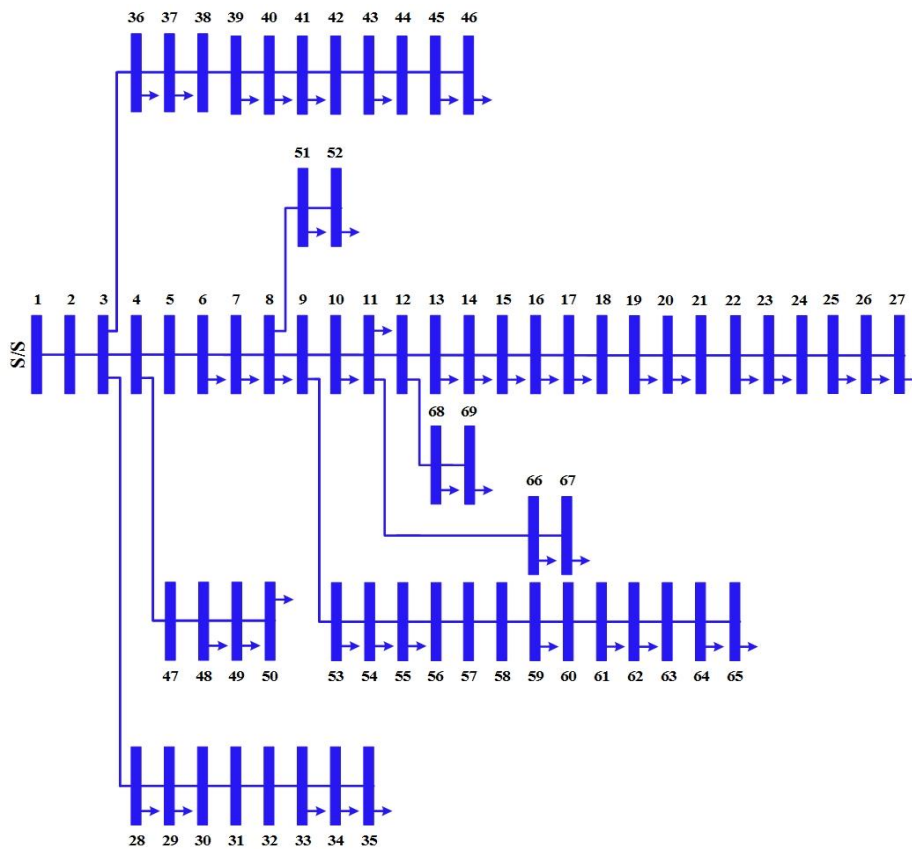
370 Figures 14 and 15 clarify a single-line schematic of these systems [34] Real and reactive power
 371 consumption for the 33-bus test system are 3715 kW and 2300 KVAR, respectively. The test system's
 372 initial power loss is 210.0794 kW, and its minimum voltage is 0.9042 pu. While 69-bus test system's
 373 active and reactive power demands are 3802 kW and 2695 KVAR, respectively. The 69-test system's
 374 initial power loss is 238.1455 kW, and its minimum voltage is 0.9046 pu.



375

376

Figure 14. Standard IEEE-33 bus test system



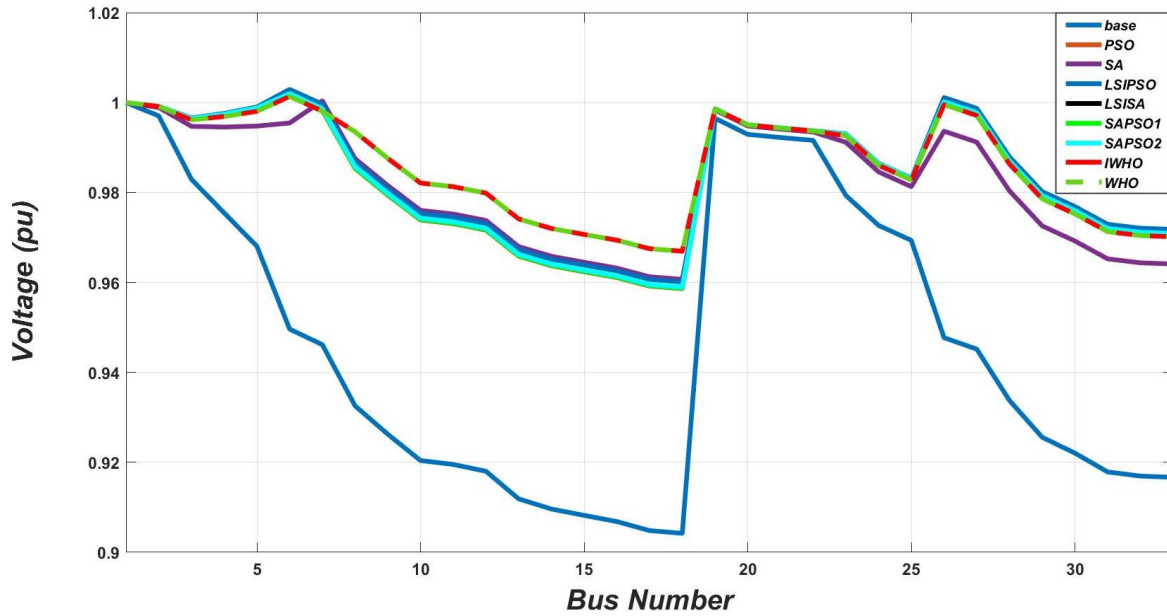
377

378

Figure 15. Standard IEEE-69 bus test system

379 5.2.1 IEEE 33-bus system

380 Figure 16 depicts the voltage profile before and after DG insertion. Bus 18 is the furthest end-
 381 point from the substation; therefore, its voltage is the least in the reference scenario (DG absence),
 382 and its value is 0.90421 pu. Without DG, buses 6 to 18 and 26 to 33 have the lowest voltage, whereas
 383 introducing DG results in a considerable voltage profile improvement within limitations (approved).
 384 Furthermore, the usage of DG yields superior outcomes in terms of power loss alleviation.



385
386 **Figure 16.** Voltage profile for IEEE-33 bus test system

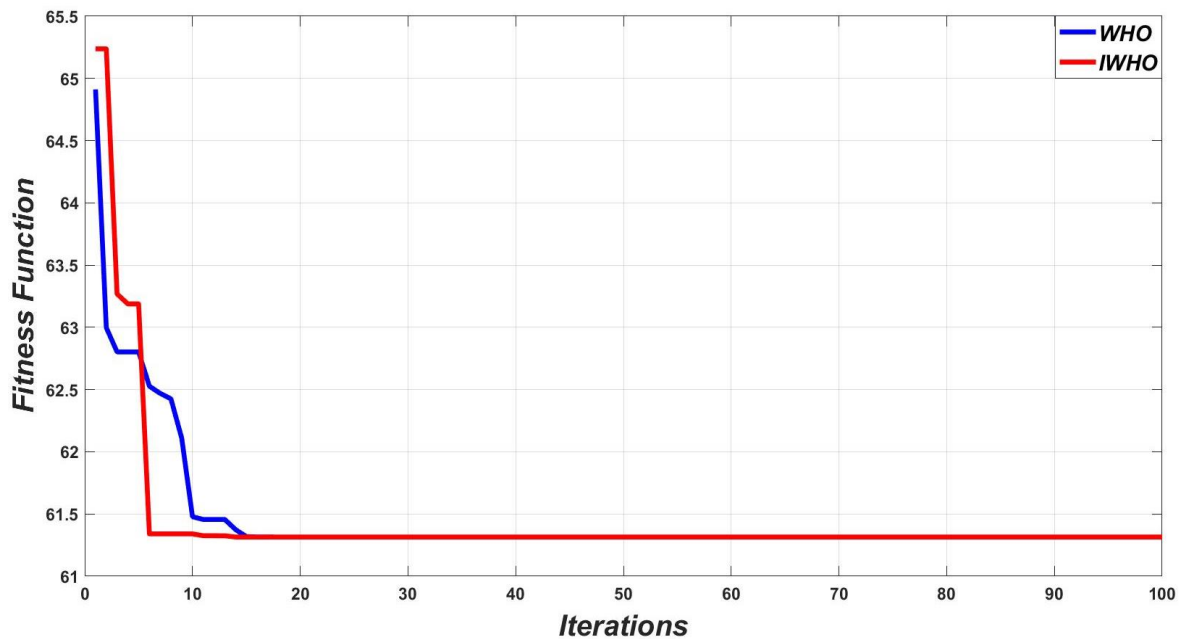
387 Table 6 displays the outcomes of the suggested approach for determining the best size, site, and
388 power factor of DG units in a 33-bus system. According to this table, the proportion of power loss
389 depression in the DS is 70.81 percent. Minimum voltages raised from 0.9042 to 0.967 pu as a result.

390 **Table 6.** The performance analysis of different algorithms in the IEEE-33 bus test system

<i>Methods</i>	<i>Power losses (kW)</i>	<i>Loss Reduction</i>	<i>Min Voltage (pu) & Bus Number</i>		<i>DG Location</i>	<i>DG Size P (KW) & Q (KVAR)</i>		<i>Itr</i>
<i>Base Case</i>	210.0794	-	0.90421	18	-	-	-	-
<i>SA</i>	70.1894	66.6%	0.95904	18	6	2935.6	1554.8	58
<i>PSO</i>	67.8228	67.7%	0.95862	18	6	2528.3	1747.9	50
<i>LSI-SA</i>	67.8118	67.7%	0.96041	18	6	2556.7	1750.0	28
<i>LSI-PSO</i>	67.8113	67.7%	0.96010	18	6	2658.8	1619.6	33
<i>SA-PSO1</i>	67.8123	67.7%	0.95872	18	6	2557.7	1748.4	10
<i>SA-PSO2</i>	67.8113	67.7%	0.95896	18	6	2511.9	1530.5	18
<i>GA</i>	72.68	64.32%	-	-	6	2831	930.5	-
<i>SAA</i>	67.75	67.89%	-	-	6	2540.84	1737.19	-
<i>GWO</i>	67.87	67.86%	-	-	6	2571.3	1794.77	20
<i>BSOA</i>	82.78	60.76%	0.9549	18	8	1857.4968	1296.54	-
<i>ALOA</i>	71.75	65.99%	0.9528	18	6	1947.756	1103.84	-
<i>HHO</i>	69.443	66.9%	0.95579	18	26	2510.01	1555.56	28
<i>HGSO</i>	68.1743	67.5%	0.9586	18	6	2653.27	1644.345	-
<i>AEO</i>	68.1698	67.55%	0.95830	18	6	2637.42	1634.526	-
<i>HSSA</i>	67.86	67.69%	-	-	6	2547.06	1777.858	-
<i>WOA</i>	78.4337	62.65%	-	-	30	1746.297	845.77	-
<i>EA</i>	67.937	67.66%	-	-	6	2528	1764.55	-
<i>Hybrid</i>	67.9	67.82%	0.9569	18	6	2482.96	1733.11	-
<i>ROA</i>	67.83	67.83%	0.95	18	6	2588.4	1785.77	17
<i>IA</i>	68.157	67.82%	-	-	6	2547.74	1778.33	-

<i>MINLP</i>	67.854	67.7%	-	-	6	2558	1765.55	-
<i>WHO</i>	61.3147	70.81%	0.967	18	6	2541.4727	1742.9416	15
<i>IWHO</i>	61.3147	70.81%	0.967	18	6	2541.4727	1742.9415	6

391 It is observed that the innovative algorithm results in the least total power loss when compared to
392 those achieved using EA [10], Hybrid approach [9], Hybrid Salp Swarm Algorithm (HSSA) [20],
393 PSO [22], SA [22], Improved Analytical (IA) [14], MINLP [14], Hybrid Loss Sensitivity Index and
394 SA (LSISA) [22], Hybrid Loss Sensitivity Index and PSO (LSIPSO) [22], Hybrid SA and PSO (SAP-
395 SO) [22], Rider Optimization Algorithm (ROA) [24], Harris Hawks Optimizer (HHO) [16], Henry
396 gas solubility optimization (HGSO) [16], whale optimization algorithms (WOA) [35], Genetic algo-
397 rithm (GA) [36], Gray wolf optimizer (GWO) [18], Simplified Analytical Approach (SAA) [17],
398 Backtracking search optimization algorithm (BSOA) [37], ALOA [19] and Artificial ecosystem-based
399 optimization (AEO) [16]. Figure 17 depicts the convergence curves of the two techniques (i.e., WHO
400 and IWHO). The findings demonstrate that the IWHO method smoothly accelerates to a correct deci-
401 sion and has stable faster convergence when compared to the WHO algorithm. The IWHO algorithm's
402 invention and notability have been proved and confirmed by identifying the best choice to attain glob-
403 al minima in a short period.



404

405 **Figure 17.** Convergence curve of the IEEE 33-bus system

406

406 5.2.2 IEEE 69-bus system

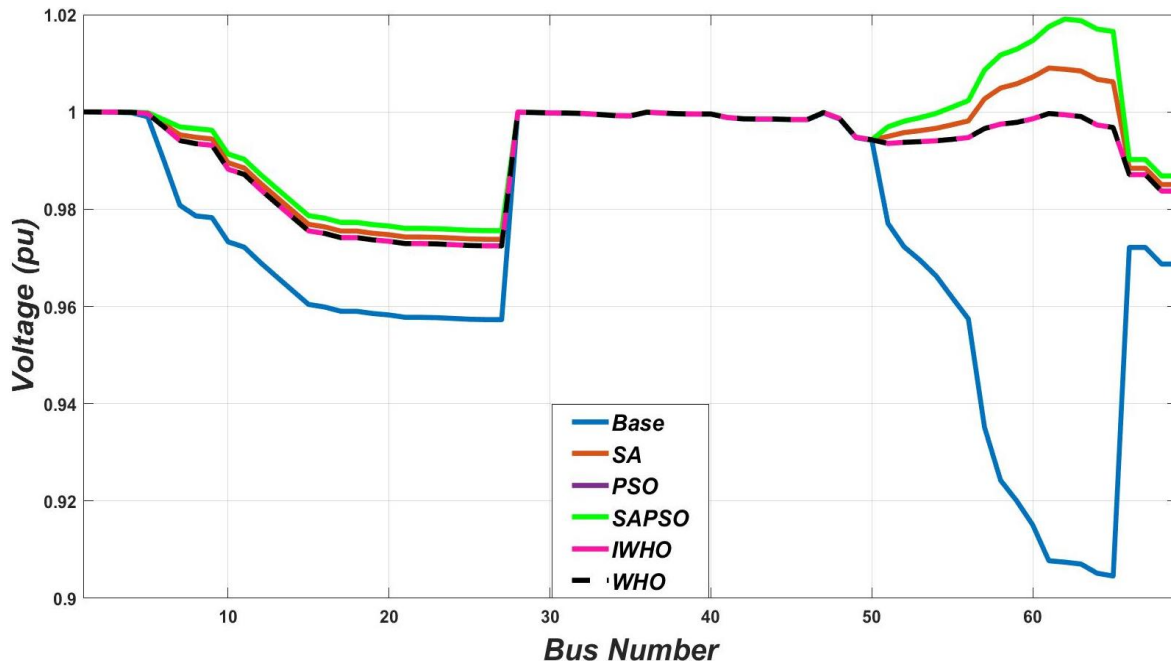
407

408

409

410

While bus 27 is the furthest end of the 69-bus system from the supply node, bus 65 have the low-
408 est voltage value 0.9046 pu because bus 61, which is linked to it is a strongly loaded point. So, it was
409 chosen as the location for the DG unit. Figure 18 displayed a significant improvement in the voltage
410 profile.



411

412 **Figure 18.** Voltage profile for IEEE-69 bus test system

413

414 Table 7 shows the outcomes of the suggested approach for determining the best size, site, and
 415 power factor of DG units in a 69-bus system. According to this table, the proportion of power loss
 depression in the DS is 90.26 percent. Minimum voltages raised from 0.9046 to 0.9725 pu as a result.

416

417

Table 7. The performance analysis of different algorithms in the IEEE-69 bus test system

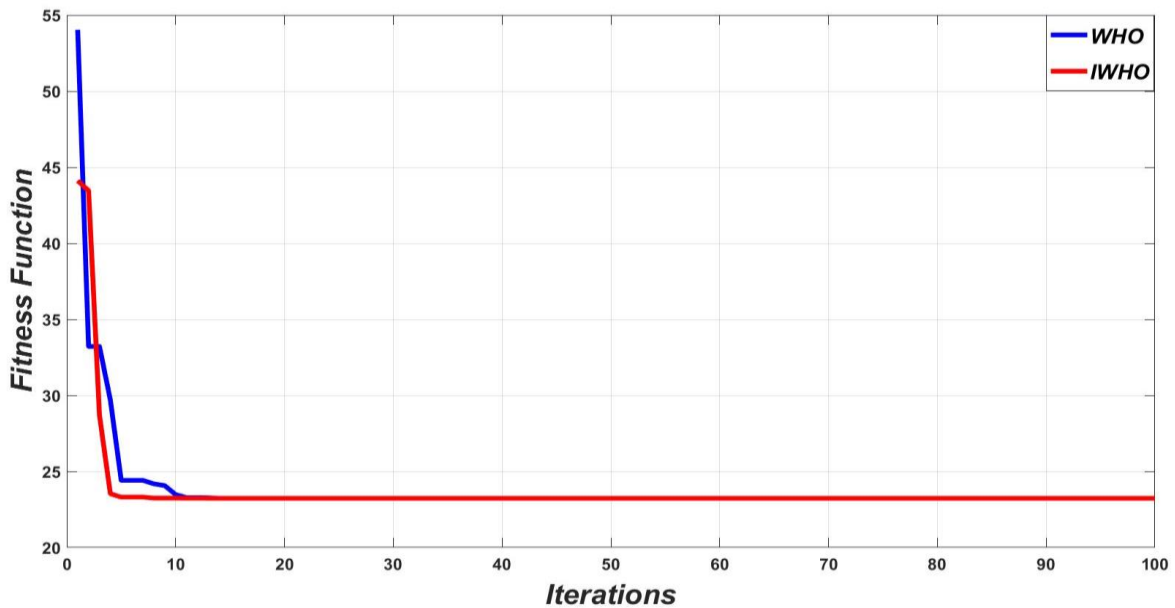
<i>Methods</i>	<i>Power losses (kW)</i>	<i>Loss Reduction</i>	<i>Min Voltage (pu) & Bus Number</i>		<i>DG Location</i>	<i>DG Size P (KW) & Q (KVAR)</i>		<i>Itr</i>
<i>Base Case</i>	238.1455	-	0.9046	65	-	-	-	-
<i>SA</i>	26.2583	88.97%	0.9727	27	61	1904.7	1571.9	39
<i>MPSO</i>	23.2358	90.24%	0.9724	27	61	1814.1	1293.3	77
<i>SAMPSO</i>	23.2378	90.24%	0.9738	27	61	1807.0	1295.3	3
<i>GA</i>	38.458	82.9	-	-	61	2047.82	673.085	-
<i>CSA</i>	52.6	76.6	-	-	61	2254	457.694	-
<i>SGA</i>	64.4	71.37	-	-	61	2548	517.39	-
<i>SAA</i>	23.18	89.7	-	-	61	1818.357	1311.74	-
<i>HHO</i>	34.65	85%	-	-	61	1879.41	1311.83	12
<i>HGSO</i>	35.71	85%	-	-	60	1695.9	1360.589	36
<i>BA</i>	52.5	76.67%	-	-	61	2100	426.42	65
<i>PSO</i>	52.5	76.67%	-	-	61	2100	426.42	75
<i>EA</i>	23.26	90.23%	-	-	61	2290	1598.429	-
<i>IA</i>	23.24	90.24%	-	-	61	1839	1283.629	-
<i>Hybrid</i>	23.19	89.7%	-	-	61	1814.4	1313.6	-
<i>MINLP</i>	23.31	90.21%	-	-	61	1828	1299.698	-
<i>MODE</i>	23.20	89.7%	-	-	61	1814.8	1290.314	-

<i>WOA</i>	27.9649	87.57%	-	-	61	1995.66	966.54	-
<i>ROA</i>	23.17	90.27%	-	-	61	1828.47	1304.78	37
<i>WHO</i>	23.178	90.26%	0.9725	27	61	1814.0767	1293.2988	10
<i>IWHO</i>	23.178	90.26%	0.9725	27	61	1814.0767	1293.2988	3

418

419 According to Table 7, the suggested algorithm has the lowest power loss when compared to the
420 Bat Algorithm (BA) [15], EA [10], Hybrid approach [9], HSSA [20], PSO [22], Modified PSO algo-
421 rithm [23], SA [22], IA [14], Mixed Integer Non- Linear Programming (MINLP) [14], Hybrid SA and
422 MPSO (SAMPSO) [23], Rider Optimization Algorithm (ROA) [24], HHO [16], HGSO [16], WOA
423 [35], GA [36], SAA [17], ALOA [19], Cuckoo Search algorithm (CSA), Standard GA [38] and Multi-
424 objective differential evolution (MODE) [39]. Figure 19 depicts the convergence curves of the two
425 techniques (i.e., WHO and IWHO). The findings demonstrate that the IWHO method smoothly accel-
426 erates to a correct selection and has stable faster convergence when compared to the WHO algorithm.
427 The IWHO algorithm's invention and notability have been proved and confirmed by identifying the
428 best option to attain global minima in a short period after 3 iterations.

429



430

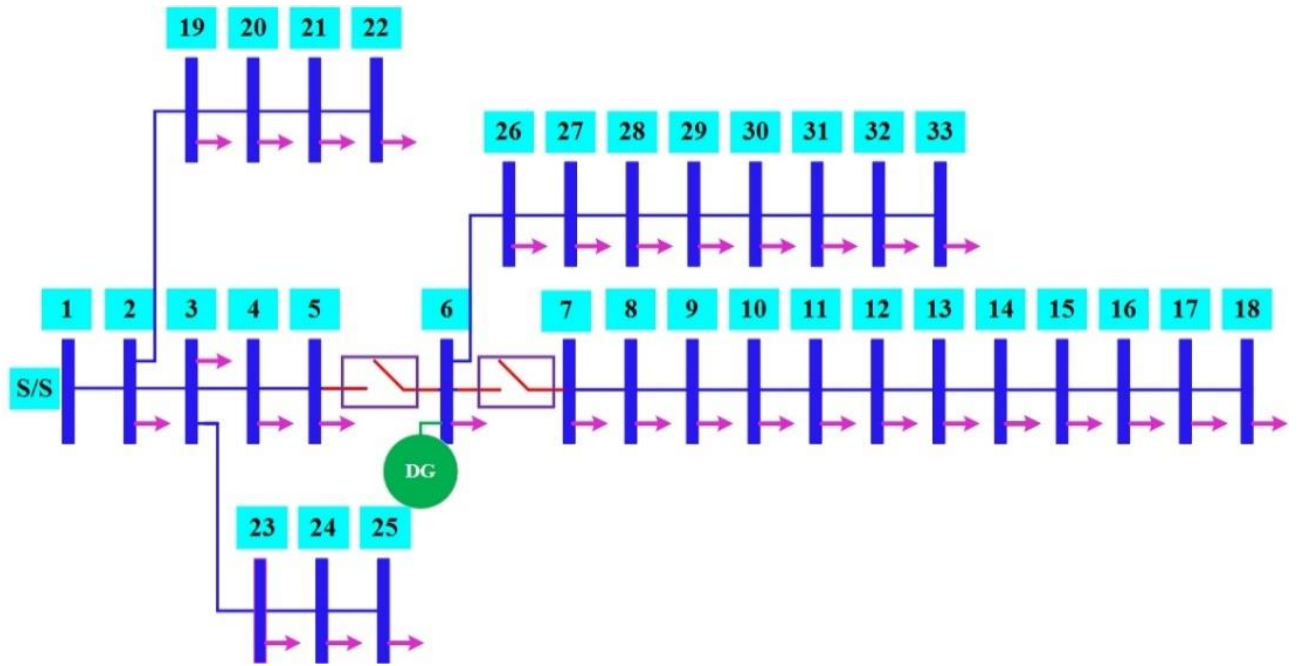
431 **Figure 19.** Convergence curve of the IEEE 69-bus system

431

432 5.3. Reliability Analysis

433 The DG incorporation can improve system reliability as DG can be actively involved in system
434 restoration. The reliability improvement can be maximized if DG units are allocated properly with
435 automatic recloser (AR). AR is a safeguard device that can identify a defect and open it for a pre-
436 programmed period before shutting automatically and without the intervention of a human aspect.
437 Figures 20 and 21 show the modified IEEE 33 & 69 bus test models, including DG and AR. Automat-

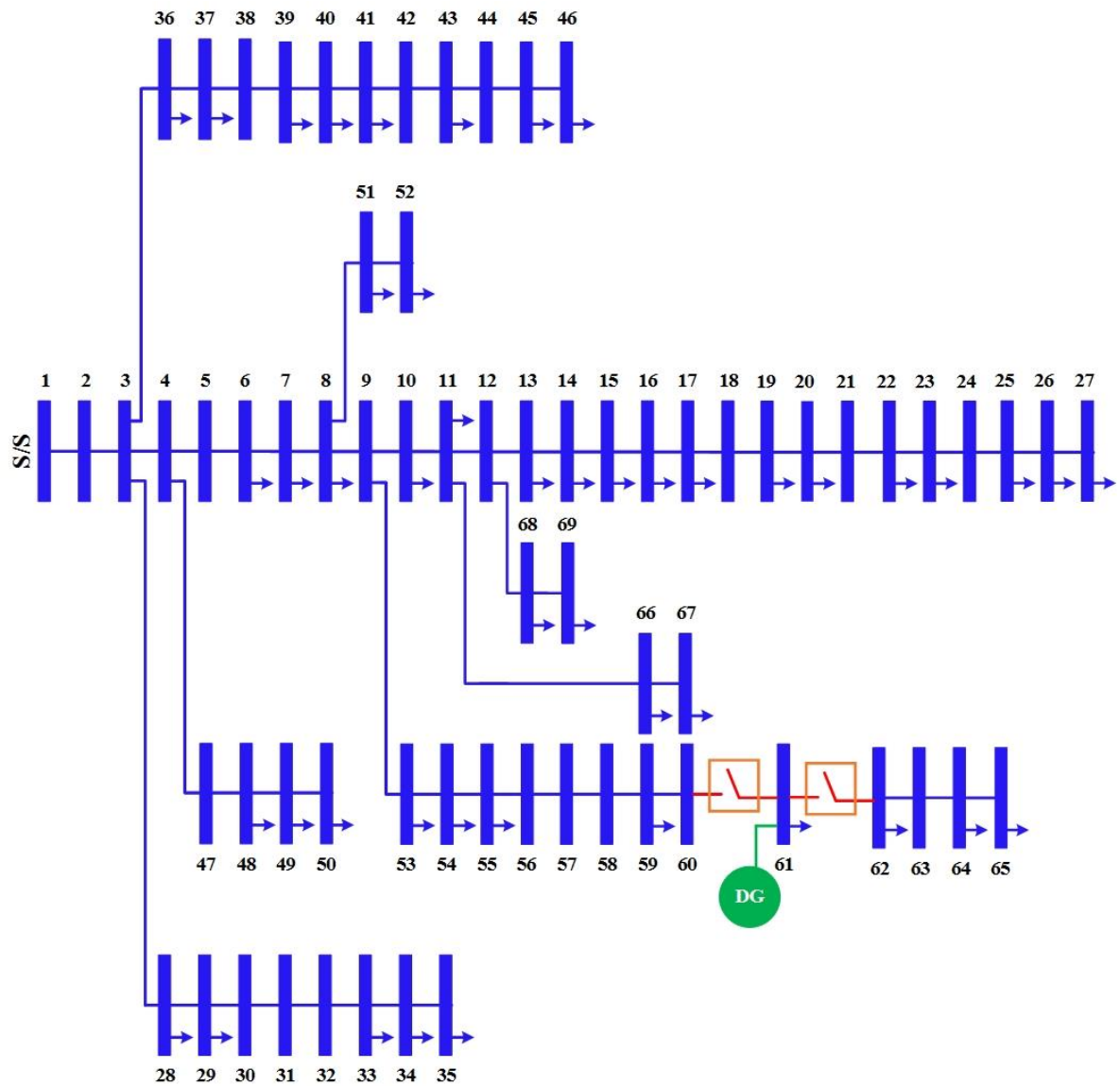
438 ic reclosers/CBs must be used when installing a DG in the DS; otherwise, there'd be no avail because
439 the fault would undoubtedly prevent the DG units from connecting during outages.



440

441

Figure 20. A modified IEEE 33 bus test



442

443

444

445

446

447

448

449

450

451

Figure 21. A modified IEEE 69 bus test

A five reliability indicators CAIDI, SAIFI, SAIDI, ASAI, and ENS are used here to assess the system reliability. Tables 4 and 5 explain the reliability indices for IEEE 33 & 69 bus systems in the base case after applying automatic recloser and applying a dual AR and DG. By comparisons: SAIFI is decreased, SAIDI is decreased, CAIDI is decreased, ASAI is increased and ENS is decreased, which means that the test systems reliability is improved as indicated in figures 22 & 23.

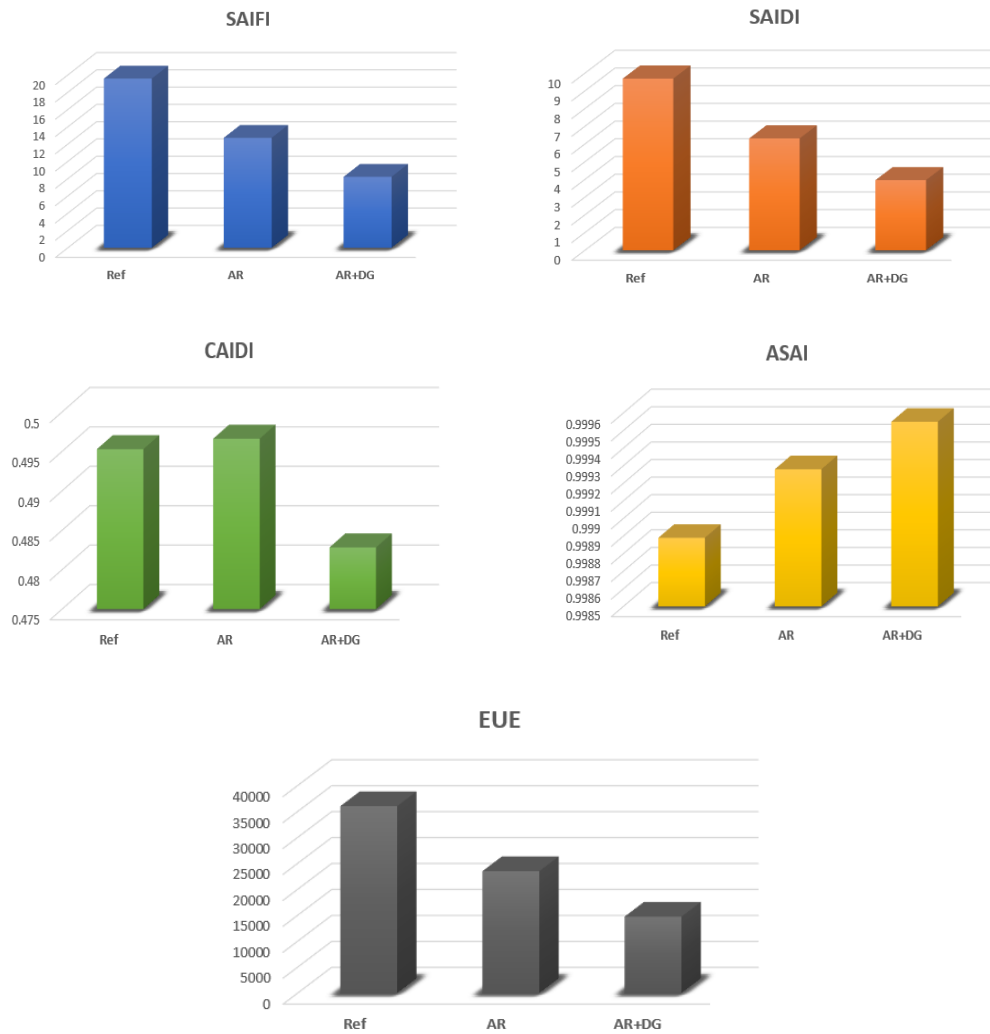
Table 8. Reliability indices for IEEE - 33 bus system

Scenario	SAIFI	SAIDI	CAIDI	ASAI	ENS
BASE	19.576	9.6957	0.49529	0.99889	36019.650
AR	12.7202	6.3171	0.49662	0.99928	23490.465

9

3

452



453

Figure 22. Comparative results of IEEE-33 system reliability

454

Table 9. Reliability indices for IEEE - 69 bus system

Scenario	SAIFI	SAIDI	CAIDI	ASAI	ENS
BASE	19.609	57.7215	2.9436	0.99341	215927.91
AR	18.1781	52.7577	2.9083	0.99398	197296.90
AR+DG	10.4966	30.5274	2.9023	0.99652	116230.16

455

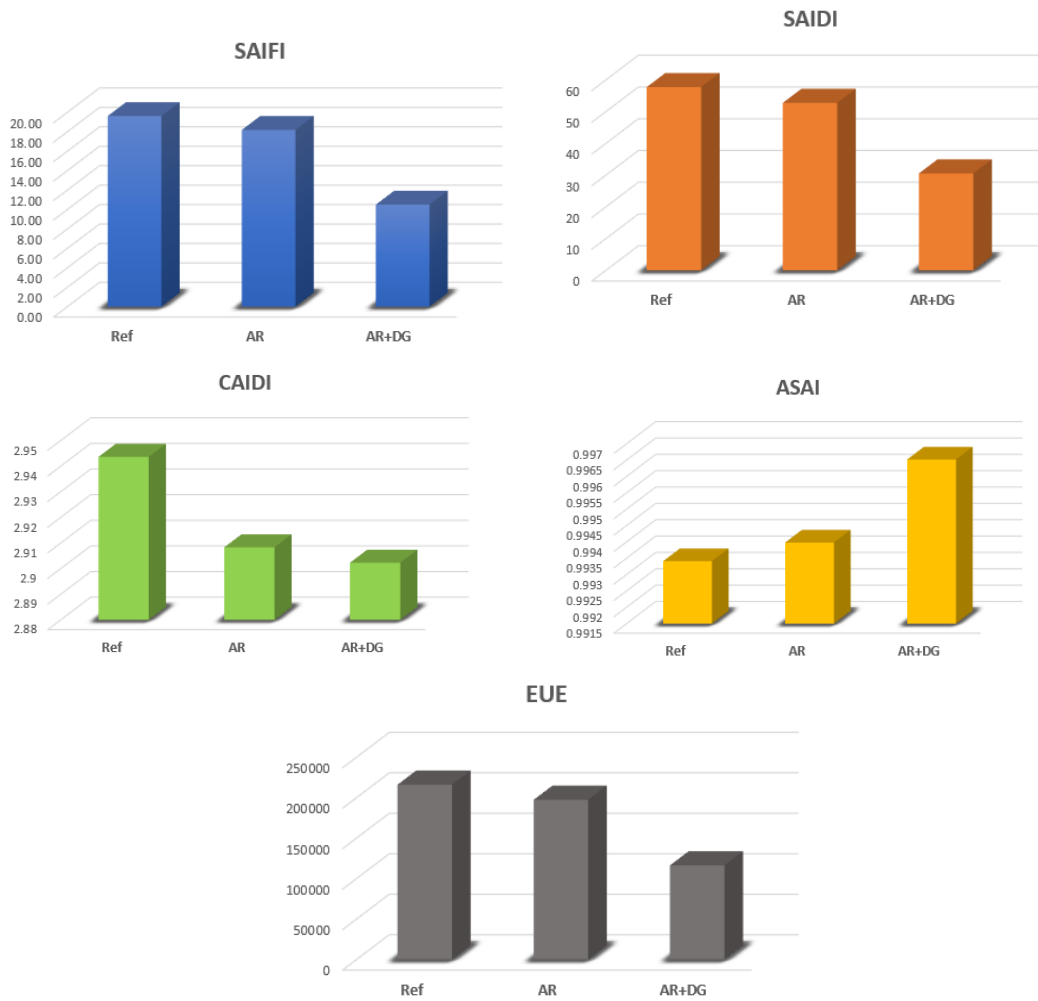


Figure 23. Comparative results of IEEE-69 system reliability

456

457 **6. Conclusions**

458 An effective optimizer called IWHO has been developed here to mend the performance of the
 459 original WHO, which was recently published and applied for the optimal site and size of DGs to slash
 460 the operational losses, boost the voltage profile, and raise the system reliability. The IWHO is created
 461 to defeat the weaknesses of the traditional WHO by meliorative the poise between the reconnoitring
 462 and utilization and hurry the algorithm convergence. The performance of the developed IWHO algo-
 463 rithm has been verified using various standards of the IEEE 33-bus and IEEE 69-bus test systems and
 464 compared with some meta-heuristic methods to discover its notability. From the findings, it can be
 465 seen that the IWHO algorithm lessened the objective function better than other comparative metaheu-
 466 ristic techniques. The simulated results confirm that the IWHO outperforms other compared tech-
 467 niques for solving ODGs problems with optimal power factors in terms of robustness and effective-
 468 ness. Lastly, the reliability evaluation is a vital component of distribution system design and planning,
 469 and the developed procedure is mainly designed to replicate the random nature of the system and
 470 power failure. The acquired findings demonstrate that the technique can guess the probability density

471 function (PDF) of several reliability indices with the necessary precision for systems in the presence
472 and absence of DGs. Because the DG units may actively participate in system recuperation, incorpo-
473 ration of them raises the system reliability. The reliability improvement can be maximized if DG units
474 are allocated properly.

475

476 **Conflicts of Interest:** The authors declare no conflict of interest.

477

478 **Acknowledgements**

479 The author (Hossam M. Zawbaa) thanks the European Union's Horizon 2020 research and Enterprise
480 Ireland for their support under the Marie Skłodowska-Curie grant agreement No. 847402.

481

482 **References**

- 483 [1] Elattar, Ehab E., and Salah K. Elsayed. "Optimal location and sizing of distributed generators
484 based on renewable energy sources using modified moth flame optimization technique." *IEEE*
485 *Access* 8 (2020): 109625-109638.
- 486 [2] Oree, Vishwamitra, Sayed Z. Sayed Hassen, and Peter J. Fleming. "Generation expansion
487 planning optimisation with renewable energy integration: A review." *Renewable and Sustainable*
488 *Energy Reviews* 69 (2017): 790-803.
- 489 [3] Huda, AS Nazmul, and R. Živanović. "Large-scale integration of distributed generation into
490 distribution networks: Study objectives, review of models and computational tools." *Renewable*
491 *and Sustainable Energy Reviews* 76 (2017): 974-988.
- 492 [4] Baran, M. E., H. Hooshyar, Z. Shen, J. Gajda, and K. M. M. Huq. "Impact of high penetration
493 residential PV systems on distribution systems." In *2011 IEEE Power and Energy Society*
494 *General Meeting*, pp. 1-5. IEEE, 2011.
- 495 [5] Dugan, Roger C., and Snuller K. Price. "Issues for distributed generation in the US." In *2002*
496 *IEEE Power Engineering Society Winter Meeting. Conference Proceedings (Cat. No.*
497 *02CH37309)*, vol. 1, pp. 121-126. IEEE, 2002.
- 498 [6] Walling, R. A., Robert Saint, Roger C. Dugan, Jim Burke, and Ljubomir A. Kojovic. "Summary
499 of distributed resources impact on power delivery systems." *IEEE Transactions on power*
500 *delivery* 23, no. 3 (2008): 1636-1644.
- 501 [7] Liu, Y., Jovan Betic, B. Kroposki, J. De Bedout, and W. Ren. "Distribution system voltage
502 performance analysis for high-penetration PV." In *2008 IEEE Energy 2030 Conference*, pp. 1-8.
503 IEEE, 2008.

- 504 [8] Eltawil, Mohamed A., and Zhengming Zhao. "Grid-connected photovoltaic power systems:
505 Technical and potential problems—A review." *Renewable and sustainable energy reviews* 14,
506 no. 1 (2010): 112-129.
- 507 [9] Kansal, Satish, Vishal Kumar, and Barjeev Tyagi. "Hybrid approach for optimal placement of
508 multiple DGs of multiple types in distribution networks." *International Journal of Electrical
509 Power & Energy Systems* 75 (2016): 226-235.
- 510 [10] Mahmoud, Karar, Naoto Yorino, and Abdella Ahmed. "Optimal distributed generation allocation
511 in distribution systems for loss minimization." *IEEE Transactions on Power Systems* 31, no. 2
512 (2015): 960-969.
- 513 [11] Essallah, Sirine, Adel Khedher, and Adel Bouallegue. "Integration of distributed generation in
514 electrical grid: Optimal placement and sizing under different load conditions." *Computers &
515 Electrical Engineering* 79 (2019): 106461.
- 516 [12] Abdul Kadir, Aida Fazliana, Tamer Khatib, Loo Soon Lii, and Elia Erwani Hassan. "Optimal
517 placement and sizing of photovoltaic based distributed generation considering costs of operation
518 planning of monocrystalline and thin-film technologies." *Journal of Solar Energy Engineering*
519 141, no. 1 (2019).
- 520 [13] Truong, Khoa H., Perumal Nallagownden, Irraivan Elamvazuthi, and Dieu N. Vo. "A quasi-
521 oppositional-chaotic symbiotic organisms search algorithm for optimal allocation of DG in radial
522 distribution networks." *Applied Soft Computing* 88 (2020): 106067.
- 523 [14] Kaur, Sandeep, Ganesh Kumbhar, and Jaydev Sharma. "A MINLP technique for optimal
524 placement of multiple DG units in distribution systems." *International Journal of Electrical
525 Power & Energy Systems* 63 (2014): 609-617.
- 526 [15] Khasanov, Mansur, Salah Kamel, and Hussein Abdel-Mawgoud. "Minimizing power loss and
527 improving voltage stability in distribution system through optimal allocation of distributed
528 generation using electrostatic discharge algorithm." In *2019 21st International Middle East
529 Power Systems Conference (MEPCON)*, pp. 354-359. IEEE, 2019.
- 530 [16] Khasanov, Mansur, Salah Kamel, Marcos Tostado-Véliz, and Francisco Jurado. "Allocation of
531 photovoltaic and wind turbine based DG units using artificial ecosystem-based optimization." In
532 *2020 IEEE International Conference on Environment and Electrical Engineering and 2020 IEEE
533 Industrial and Commercial Power Systems Europe (EEEIC/I&CPS Europe)*, pp. 1-5. IEEE,
534 2020.
- 535 [17] Sa'ed, Jaser A., Mohammad Amer, Ahmed Bodair, Ahmad Baransi, Salvatore Favuzza, and
536 Gaetano Zizzo. "A simplified analytical approach for optimal planning of distributed generation
537 in electrical distribution networks." *Applied Sciences* 9, no. 24 (2019): 5446.
- 538 [18] Kamel, Salah, Ayman Awad, Hussein Abdel-Mawgoud, and Francisco Jurado. "Optimal DG
539 allocation for enhancing voltage stability and minimizing power loss using hybrid gray wolf

- 540 optimizer." *Turkish Journal of Electrical Engineering & Computer Sciences* 27, no. 4 (2019):
541 2947-2961.
- 542 [19] Ali, E. S., S. M. Abd Elazim, and A. Y. Abdelaziz. "Ant lion optimization algorithm for
543 renewable distributed generations." *Energy* 116 (2016): 445-458.
- 544 [20] Abdel-mawgoud, Hussein, Salah Kamel, Juan Yu, and Francisco Jurado. "Hybrid Salp Swarm
545 Algorithm for integrating renewable distributed energy resources in distribution systems
546 considering annual load growth." *Journal of King Saud University-Computer and Information
547 Sciences* (2019).
- 548 [21] Samala, Rajesh Kumar, and Mercy Rosalina Kotapuri. "Optimal allocation of distributed
549 generations using hybrid technique with fuzzy logic controller radial distribution system." *SN
550 Applied Sciences* 2, no. 2 (2020): 1-14.
- 551 [22] Ali, Mohammed Hamouda, Mohammed Mehanna, and Elsaied Othman. "Optimal planning of
552 RDGs in electrical distribution networks using hybrid SAPSO algorithm." *International Journal
553 of Electrical and Computer Engineering (IJECE)* 10, no. 6 (2020): 6153-6163.
- 554 [23] Ali, Mohammed Hamouda, Mohammed Mehanna, and Elsaied Othman. "Optimal Network
555 Reconfiguration Incorporating with Renewable Energy Sources in Radial Distribution
556 Networks." *International Journal of Advanced Science and Technology*, Vol. 29, No. 12s,
557 (2020), pp. 3114 – 3133.
- 558 [24] Khasanov, Mansur, Salah Kamel, Claudia Rahmann, Hany M. Hasanien, and Ahmed Al-Durra.
559 "Optimal distributed generation and battery energy storage units integration in distribution
560 systems considering power generation uncertainty." *IET Generation, Transmission &
561 Distribution* (2021).
- 562 [25] Billinton, Roy, and Peng Wang. "Teaching distribution system reliability evaluation using Monte
563 Carlo simulation." *IEEE Transactions on Power Systems* 14, no. 2 (1999): 397-403.
- 564 [26] Transmission, D. "Committee et al.,“." *Ieee guide for electric power distribution reliability
565 indices,*” *IEEE Std* (2003): 1366-2003.
- 566 [27] Naruei, Iraj, and Farshid Keynia. "Wild horse optimizer: a new meta-heuristic algorithm for
567 solving engineering optimization problems." *Engineering with Computers* (2021): 1-32.
- 568 [28] Gandomi, Amir Hossein, Xin-She Yang, and Amir Hossein Alavi. "Cuckoo search algorithm: a
569 metaheuristic approach to solve structural optimization problems." *Engineering with
570 computers* 29.1 (2013): 17-35.
- 571 [29] Long, Wen, et al. "A new hybrid algorithm based on grey wolf optimizer and cuckoo search for
572 parameter extraction of solar photovoltaic models." *Energy Conversion and Management* 203
573 (2020): 112243.
- 574 [30] Dehghani, Mohammad, Zeinab Montazeri, and Štěpán Hubálovský. "GMBO: Group Mean-
575 Based Optimizer for Solving Various Optimization Problems." *Mathematics* 9.11 (2021): 1190.

- 576 [31] Mirjalili, Seyedali, Seyed Mohammad Mirjalili, and Andrew Lewis. "Grey wolf
577 optimizer." *Advances in engineering software* 69 (2014): 46-61.
- 578 [32] Kaur, Satnam, et al. "Tunicate Swarm Algorithm: A new bio-inspired based metaheuristic
579 paradigm for global optimization." *Engineering Applications of Artificial Intelligence* 90 (2020):
580 103541.
- 581 [33] Dhiman, Gaurav, and Vijay Kumar. "Seagull optimization algorithm: Theory and its applications
582 for large-scale industrial engineering problems." *Knowledge-Based Systems* 165 (2019): 169-
583 196.
- 584 [34] Satya Krishna Pothapragada, Pruthvi Raj Mandala, Srikanth Reddy Hanumandla, Dr. P. Ravi.
585 (2020). Implementation of expert methodology for optimal reconfiguration in electrical
586 distribution system to minimize I²R Losses. *International Journal of Advanced Science and*
587 *Technology*, Vol. 29, No. 3s, pp. 242-254.
- 588 [35] VC, Veera Reddy. "Optimal renewable resources placement in distribution networks by
589 combined power loss index and whale optimization algorithms." *Journal of Electrical Systems*
590 *and Information Technology* 5, no. 2 (2018): 175-191.
- 591 [36] Hassan, Amal A., Faten H. Fahmy, Abd El-Shafy A. Nafeh, and Mohamed A. Abu-elmagd.
592 "Genetic single objective optimisation for sizing and allocation of renewable DG
593 systems." *International Journal of Sustainable Energy* 36, no. 6 (2017): 545-562.
- 594 [37] El-Fergany, Attia. "Optimal allocation of multi-type distributed generators using backtracking
595 search optimization algorithm." *International Journal of Electrical Power & Energy Systems* 64
596 (2015): 1197-1205.
- 597 [38] Tan, W. S., M. Y. Hassan, M. S. Majid, and H. A. Rahman. "Allocation and sizing of DG using
598 cuckoo search algorithm." In *2012 IEEE international conference on power and energy (PECon)*,
599 pp. 133-138. IEEE, 2012.
- 600 [39] Behera, Snigdha R., and Bijaya K. Panigrahi. "A multi objective approach for placement of
601 multiple DGs in the radial distribution system." *International Journal of Machine Learning and*
602 *Cybernetics* 10, no. 8 (2019): 2027-2041.
- 603